*J Toxicol Pathol 2025; 38: 93–111*

**Technical Report**

# Histopathology of incidental non-neoplastic findings in transgenic CByB6F1-Tg(HRAS)2Jic mice used in toxicity studies

Marcia E Pereira Bacares[1]*, Edward L Stevens[1], Victoria Laast[1]*, Vimala Vemiredi[1], Hibret A Adissu[1], and Mark G Mense[1]

[1]Labcorp Early Development Laboratories, Inc., 3635 Concorde Parkway, Suite 100, Chantilly, VA, 20151, USA

**Abstract:** This technical report presents a collection of illustrative images and concise descriptions of non-neoplastic microscopic findings noted in transgenic CByB6F1-Tg(HRAS)2Jic (Tg.rasH2) mice from 26-week-carcinogenicity studies. A unique finding in the Tg.rasH2 strain was the skeletal muscle myopathy observed in nearly all animals, particularly affecting the *femoralis* and *pectoralis* muscles, diaphragm, and subcutaneous muscles. Pigment was noted in various organs, particularly in the spleen due to the C57BL/6J background. Mononuclear and/or mixed cell inflammatory infiltrates occurred in various tissues, with or without secondary changes, similar to other rodent and non-rodent laboratory species. Vascular anomalies were sporadically noted, mainly in the uterus. Other notable findings included extramedullary hematopoiesis in the spleen; alveolar macrophage infiltrate (often with eosinophilic crystals) in the lung; and proliferative findings in several tissues, such as the lung (bronchiolo-alveolar hyperplasia), adrenal cortex (subcapsular hyperplasia), and uterus (cystic-endometrial hyperplasia). This paper also includes illustrations of other less frequently incidental findings. The information presented in this manuscript aims to serve as a valuable reference for pathologists and researchers and expected to offer contextual insights for carcinogenicity and other toxicological studies utilizing this animal model. (DOI: 10.1293/tox.2024-0037; J Toxicol Pathol 2025; 38: 93–111)

**Key words:** rasH2-Tg mouse, spontaneous, incidental, background, histopathology, carcinogenicity

The rasH2® mouse strain is the trade name for genetically manipulated CByB6F1-Tg(HRAs)2Jic mice developed as a rodent test system for 26-week carcinogenicity studies. The use of this mouse model is recognized by several global regulatory authorities and has gained wide acceptance for use in carcinogenicity studies in the pharmaceutic industry[1, 2], based on the experience at our contract research laboratory. The rasH2-Tg mouse was engineered in Japan by Nomura and his team[3] with the HRAS(c-Ha-ras) gene, a prototype prepared by removal of the point mutation sites from two HRAS (c-Ha-ras) genes obtained from human malignant melanoma and human urinary bladder carcinoma, followed by their recombination; thus, the model carries multiple copies of the human c-Ha-ras gene with their own promoter and enhancer[2]. The rasH2-Tg strain is used for 26-week carcinogenicity studies to assess hazard identification of pharmaceutical candidates[4, 5]. To accurately provide pathological evaluation for safety risk assessment in studies, pathologists must be able to distinguish spontaneous background findings in laboratory animals from those that are induced by test article(s). Spontaneous tumors and N-Nitroso-N-methylurea (MNU)-induced neoplastic findings are well documented in this strain[6–14]. However, fewer published reports are available with comprehensive representative images for pathologists to use as a reference to identify non-neoplastic, background histopathological findings in rasH2-Tg mice[15–17]. The purpose and scope of this technical report is to provide a collage of illustrative images and brief descriptions of non-neoplastic findings in rasH2-Tg mice organized by system and tissues queried from background data from controls collected from Labcorp® Laboratories. The incidence of the background findings is beyond the objective and scope of this technical report, and the reader is referred to the extensive list of references provided should more information be desired on this topic.

Background data were queried from control mice from 51 carcinogenicity studies (26-week) conducted at Labcorp Early Development Laboratories (Labcorp), USA during 2013 to 2023. Data reported originated from 3,575 (1,800 males and 1,775 females) CByB6F1-Tg(HRAS)2Jic (+/− hemizygous c-Ha-ras) mice obtained from Taconic Biosciences (Germantown, NY, USA) with the brand name rasH2® mouse, and assigned to saline and/or vehicle control groups. The numbers of animals, procedures, and experimental design for each study were reviewed and approved by the Labcorp Institutional Animal Care and Use Com-

Received: 18 April 2024, Accepted: 20 September 2024
Published online in J-STAGE: 20 November 2024
Corresponding authors:
ME Pereira Bacares (e-mail: marcia.pereirabacares@labcorp.com);
V Laast (e-mail: victoria.laast@labcorp.com)

mittees. Animal care and use was performed in accordance with the Guide for Care and Use of Laboratory Animals at AAALAC International accredited programs. The studies were conducted in compliance with principles of Good Laboratory Practice Standards as set forth in the U.S. Food and Drug Administration's Good Laboratory Practice Regulations (Part 58 of 21 CFR-Code of Federal Regulations).

Mice were housed in polycarbonate cages with hardwood chip bedding. Females were group-housed (up to three animals/cage) and males were individually housed. The type of bedding and cage (stainless steel) were changed if needed for behavioral or health reasons. Temperature, humidity, and light cycle were monitored in accordance with Labcorp's standard operating procedures. Animals had free access to food and water *ad libitum*. Mice were humanely euthanized with isoflurane followed by exsanguination. Comprehensive necropsy was performed on all animals at study termination or on the day of the death for animals found dead or euthanized in moribund condition prior to study termination. Organs were fixed in the appropriate fixative, which were neutral buffered formalin for most soft tissue, including gross observations, modified Davidson's solution for ocular tissues, testis and epididymis for males; and bones (with marrow) were immersed in decalcification solution, embedded in paraffin, and hematoxylin and eosin (H&E) stained sections at a nominal 5 µm thick were prepared for microscopic examination. Microscopic data was recorded by a board-certified study pathologist using data capture system Pristima® system (Xybion, Princeton, NJ, USA). Eighty images of selected slides were scanned for photomicrography. The whole slide images were generated using the Leica®/Aperio AT2 Digital Slide Scanner (Leica/Aperio Digital Scanner, Vista, CA, USA) and scanned at 40× magnification. Images were stored and managed using Leica®/Aperio eSlide Manager v12.4. All images presented in this technical report originated from negative control (untreated) groups only. A listing of 80 selected findings observed in untreated saline and/or control rasH2-Tg mice at our laboratory was captured. Selected findings ranged from those frequently observed to those infrequently present and were limited to non-neoplastic findings in rasH2-Tg mice from 26-week carcinogenic studies. Brief descriptions or explanations for these findings are provided in the figure legends.

Myopathy: A finding unique to rasH2-Tg mouse is the skeletal muscle myopathy (Fig. 78) found in almost all rasH2-Tg mice, with incidence ranging between 81 and 100%[4, 7, 16, 18, 19]. Although this finding occurs with higher incidence in older animals, it can be seen in animals as young as 10 weeks old[19]. Primary changes include degeneration, necrosis, and atrophy of the myofibers with vacuolation, loss of striations, coagulation, hyalinization, increased eosinophilia, with secondary associated mononuclear or mixed inflammatory cell infiltrate and/or myocyte regeneration (myofiber basophilia and nuclear rowing)[16]. This finding is frequently noted in the skeletal muscle *femoralis* and *pectorali*[19] (Tsuchiya *et al*., 2002) but can also be present in the tongue[7, 19](Fig. 15) diaphragm, and subcutaneous skeletal muscle. To the authors' knowledge, these findings have not been reported in the heart[19]. Myopathy of the skeletal muscle occurs with variable degrees of severity, but no sex difference in incidence and severity is observed[16] and no clinical observations associated with these muscle changes have been reported in rasH2-Tg mice. Myopathy is not observed in non-transgenic/wild type CB6F1-non rasH2-Tg mice[15]. Although we consider this background finding to be the most frequent in this transgenic strain and related to the c-Ha-ras gene, we recommend recording the muscle changes in the microscopic data as standard practice to provide additional documentation for the expected phenotypic characteristics of the model. Muscle degeneration and regeneration in the esophagus is not a reported phenotypic manifestation of the strain[7, 19], and the sporadic finding of myocyte degeneration/regeneration (often with focal distribution) in the esophagus is noted most often in oral gavage studies in our experience, and typically attributed to the gavage-related procedure (Fig. 16).

Vascular anomaly: Another unique finding in rasH2-Tg mice is vascular anomaly (Fig. 57) noted sporadically in various organs, with higher incidence in females, and most often in the uterus[13, 16]. Vascular anomalies are characterized by thick walled, blood containing vessels lined by well-differentiated endothelial cells[16]. Vascular anomalies of the uterine serosa can progress to proliferative lesions, such as hemangiosarcoma[13, 16], and therefore should be considered a pre-neoplastic finding[13]. Vascular anomalies should be differentiated from other vascular lesions, including thrombosis of the mesenteric arteries, a finding with higher incidence in male rasH2-Tg mice as compared with females[16].

Pigmentation: Because the rasH2-Tg mouse is a hemizygous transgenic strain carrying the c-Ha-ras oncogene with the gene's promotor/enhancer embedded within the genetic background of a BALB/cByJ × C57BL/6J F1 mouse[20], background histologic findings reported in C57BL/6J and BALB/cByJ mice can also be observed and are expected in the Tg.rasH2 strain. The observation of pigment in a variety of tissues is a good example and is frequent in the Tg.rasH2 strain due to the C57BL/6J background. Pigment is often noted in the spleen (Fig. 8) with the macroscopic correlate of discolored or dark areas observed in the spleen. Pigment can also be seen in a variety of other tissues, including the meninges of the brain (Fig. 72), paranasal sinus (Fig. 14) in the nasal turbinates, heart valves (Fig. 2), parathyroid (Fig. 67) and adrenal glands, among others (Fig. 30, Fig. 59, Fig. 61). Pigment in the adrenal gland has been reported more frequently in female rasH2-Tg mice as compared with males[7].

Extramedullary hematopoiesis: Extramedullary hematopoiesis is frequent in the spleen (Fig. 9) of the Tg.rasH2 strain, with a higher incidence in females as compared with males[16], similar to the incidence of the parent strains of C57BL/6J and BALB/cByJ mice[21–23]. Extramedullary hematopoiesis can also occur in the liver (Fig. 33) in rasH2-Tg mice. In the spleen, extramedullary hematopoiesis may occasionally correlate with macroscopic observations of

enlarged organ[16]. Increased extramedullary hematopoiesis in the spleen and other tissues can often be observed in association with hemorrhage and/or blood loss, inflammation, or malignant neoplasms, notably hemangiosarcoma[16].

Inflammatory lesions: Other frequent findings, though not strain related, include mononuclear cell, mixed cell, and neutrophilic infiltrates in various organs, and alveolar histiocyte/macrophage infiltrates in the lung. Mononuclear cell infiltrates which seem to be more frequent than mixed cell or neutrophilic infiltrates (Fig. 10, Fig. 24, Fig. 60) in our experience, may be observed in various tissues (Fig. 1, Fig 11, Fig. 17, Fig. 25, Fig. 27, Fig. 42, Fig. 44, Fig. 47, Fig. 50, Fig. 54, Fig. 62, Fig. 74, Fig. 76, and Fig. 77), and typically are not accompanied by other morphologic changes in the infiltrated tissue. Mixed cell infiltrates (Fig. 19, Fig. 20, Fig. 26, Fig. 38, Fig. 66, Fig. 75, Fig. 79) seem to be less frequent, and unlike mononuclear cell infiltrates, it is not uncommon to observe associated degenerative changes in cells adjacent to the infiltrate, such as degenerate hepatocytes in the liver (Fig. 32). Mixed cell and/or neutrophilic infiltrates are not uncommon in the glandular stomach (Fig. 18) at the limiting ridge and may be associated with eosinophilic globules/eosinophilic hyaline inclusions of the overlying glandular epithelial cells[16], dilation of the glands[7], and/or gastric mucosal hyperplasia (Fig. 20, Fig. 22) (focal or diffuse). Mixed cell infiltrates, often with a predominance of neutrophils, can be seen in the cervix and vagina lumen (Fig. 60) of female rasH2-Tg mice. Neutrophils are frequently present in the vaginal cytology of mice in metestrus and diestrus[24]. Neutrophils may also be present in the gallbladder mucosa. Alveolar histiocyte/macrophage infiltrates are frequent in the lung (Fig. 11) (especially in females) and may be more frequently associated with bronchioloalveolar proliferative lesions (hyperplasia, adenomas, or carcinoma)[16]. The alveolar histiocytes/macrophages have an abundant, intensely acidophilic cytoplasm[16] and are occasionally accompanied by eosinophilic, hyalinized crystals noted in the cytoplasm of macrophages or free within alveoli[16]. This finding is also sometimes observed in C57BL/6 mice[25]. Additionally, macrophages were noted in the lymph nodes (Fig. 4) with or without sinus erythrocytes (Fig. 5). Mixed cell inflammation was an uncommon finding in some tissues (Fig. 21, Fig. 45, Fig. 51).

Age-related lesions: Rodent progressive cardiomyopathy in the heart (Fig. 3), chronic progressive nephropathy in the kidney (Fig. 40), amyloid-like material in the nasal cavity (Fig. 13), and chondromucinous degeneration of the articular cartilage in the sternum (Fig. 80) are some background findings often considered as age related, similar to other wild type rodent strains. Rodent progressive cardiomyopathy, a well characterized background finding in the heart of various laboratory rodent strains, differs from the skeletal muscle myopathy documented in the rasH2-Tg mouse strain in that the finding in the heart occur sporadically and seems to be age-related in contrast with the skeletal muscle myopathy which occurs universally in almost all animals, including younger mice. Findings in the kidney considered within the spectrum of chronic progressive nephropathy include basophilic cortical tubules, hyaline casts, mineralization (Fig. 43), tubular vacuolation (Fig. 39), and mononuclear cell infiltrates (Fig. 42). Chronic progressive nephropathy was less prominent in rasH2-Tg when compared CD-1® mice; and tubular vacuolation (Fig. 39) seems to be more frequent in Tg.rasH2 males as compared with females[7]. Decidual reaction in the uterus (Fig. 58) were observed in our rasH2-Tg studies.

Degenerative lesions: Degenerative changes may occur virtually in any tissue in rasH2-Tg mice, with notable examples of degeneration of the X zone in the adrenal gland of females (Fig. 69); and degeneration and atrophy of seminiferous tubules in the testis (Fig. 46) and cellular debris in the epididymis (Fig. 48) of males, both of which are sometimes associated with sperm granulomas (Fig. 49)[7, 16]. Other occasional degenerative changes noted in Labcorp studies included erosion in the glandular stomach (Fig. 23), tension lipidosis (Fig. 34), hepatocyte vacuolation (Fig. 31), and focal necrosis in the liver (Fig. 36), and acinar cell vacuolation in the pancreas (Fig. 28). Cystic lesions were also observed sporadically in rasH2-Tg mice, and similar to other rodent strains, were noted in a variety of tissues, including the pituitary (Fig. 63), thyroid (Fig. 65), parathyroid (Fig. 67), liver (biliary cyst), spinal cord (squamous cyst, – Fig. 73), ovary (Fig. 55), and kidney (Fig. 41). Dilation was noted in the coagulation gland (Fig. 52) and preputial gland (Fig. 53).

Proliferative lesions: In Labcorp Tg.rasH2 studies, proliferative changes were noted consistently in several tissues, albeit with variable incidence, including in the lung, thymus, glandular stomach, adrenal cortex (Fig. 70), liver, thyroid, and uterus. Adrenal cortical subcapsular hyperplasia (Fig. 68) is a frequent finding in both sexes, tends to occur with a greater incidence and severity in females[17], and reportedly does not appear to progress to neoplasia in rasH2-Tg mice[17]. Changes vary from subtle, small aggregates of spindle cells arranged parallel and/or perpendicular to the capsule to large foci of fusiform cells with rare polygonal cells (type B), arranged in nests, sometimes elevating the overlying capsule[17]. In the lung, bronchiolo-alveolar hyperplasia (Fig. 12) was noted more frequently in males and was typified by proliferation of well-differentiated epithelial cells in small papillary projections without compression or alteration of alveolar architecture and adjacent tissue[16], which differentiated the hyperplastic finding from bronchioloalveolar adenoma. Hyperplasia of the glandular gastric mucosa (Fig. 22) may occasionally be seen in rasH2-Tg mice, and the lesion may be either focal or diffuse in nature[22] and often accompanied with infiltrates of mixed inflammatory cells or neutrophils. The proliferative finding of basophilic focus in the liver (Fig. 37) was not frequent in Tg.rasH2 studies in our experience; this finding has been reported to occur with a higher incidence in males[7, 16]. These basophilic foci are typically randomly distributed, have relatively indistinct margins, and usually do not compress or have little compression of the surrounding parenchyma. The hepatocytes within these foci are arranged in normal cords, and

the cells appear more basophilic than normal[16]. Basophilic focus was also noted in the pancreas (Fig. 29). In females, cystic endometrial hyperplasia of the uterus (Fig. 56) is another frequent finding in rasH2-Tg mice[7]. In the thymus, epithelial hyperplasia (Fig. 6) was occasionally observed in our Tg.rasH2 controls, though some laboratories have reported this as a rare finding[16]. Thymic epithelial hyperplasia may be age-related, as seems to occur in thymus sections with evidence of involution, and predominantly occurs in females[26]. The finding is typified microscopically by clusters of closely associated proliferating epithelial cells with a spindle or squamous appearance[16]. Pleomorphic variations of thymic epithelial hyperplasia may have characteristics considered within the spectrum of thymoma; thus, robust hyperplastic lesions may be difficult to distinguish from early thymoma[26].

Nasal cavity lesions: In Labcorp Tg.rasH2 26-week carcinogenicity studies, nasal cavity is generally an uncommon protocol tissue for microscopic examination and is most often collected in oral gavage studies. Background microscopic findings observed in nasal turbinate sections included amyloid in the subepithelial interstitium and intracytoplasmic eosinophilic, hyaline globules/inclusions in the respiratory epithelium, both of which were noted predominantly in the nasal septum (Fig. 13). Amyloid has been reported in nasal cavity of rodents, including Tg.rasH2 mice, with more abundant deposition in older animals[27]. A detailed study by Doi *et al.* with special stains and electron microscopy showed that the eosinophilic substance of the nasal septum often called amyloid was not amyloid, but rather composed of collagen and complex carbohydrates. Regardless of the nature of the deposition, this deposit is typically not accompanied by degenerative and/or inflammatory changes. Eosinophilic globules/inclusions are homogenous hyaline material of unknown composition that accumulates in the sub-or supranuclear regions of the cytoplasm in respiratory epithelium, sustentacular cells of the olfactory epithelium, or in the submucosal glands and ducts[28] and are considered an age-related change in mice[29], with higher incidence in female rasH2-Tg mice[7].

Additional miscellaneous findings: Cholesterol granuloma (Fig. 7), thrombus (Fig. 35), ectopic thymus (Fig. 64), and lipomatous hamartoma in the brain (Fig. 71) were observed in our rasH2-Tg studies.

Although all findings described in this publication were representative of animals from control groups, background findings can also be seen in treated animals, and as in other laboratory animal species, some of the findings considered spontaneous and incidental may be exacerbated by administration of certain test articles or test agents.

**Disclosure of Potential Conflicts of Interest:** All authors are/were employees of Labcorp Early Development Laboratories at the time of their contribution to the manuscript. The authors declare no potential conflicts of interest regarding the research, authorship, or publication of this article.

**Acknowledgments:** The authors express sincere appreciation to Julie Turner for helping with historical control data base search, Steven Van Adestine and Laota Hoeft for assistance with image scanning and preparation.

## References

1. MacDonald J, French JE, Gerson RJ, Goodman J, Inoue T, Jacobs A, Kasper P, Keller D, Lavin A, Long G, McCullough B, Sistare FD, Storer R, van der Laan JW. The Alternatives to Carcinogenicity Testing Committee ILSI HESI. The utility of genetically modified mouse assays for identifying human carcinogens: a basic understanding and path forward. Toxicol Sci. **77**: 188–194. 2004. [Medline] [CrossRef]
2. Hickam S. Initial development of transgenic mouse models for carcinogenicity testing and review of the regulatory environment. Am Lab. **47**: 14–17. 2015.
3. Saitoh A, Kimura M, Takahashi R, Yokoyama M, Nomura T, Izawa M, Sekiya T, Nishimura S, and Katsuki M. Most tumors in transgenic mice with human c-Ha-ras gene contained somatically activated transgenes. Oncogene. **5**: 1195–1200. 1990. [Medline]
4. Morton D, Alden CL, Roth AJ, and Usui T. The Tg rasH2 mouse in cancer hazard identification. Toxicol Pathol. **30**: 139–146. 2002. [Medline] [CrossRef]
5. Bogdanffy MS, Lesniak J, Mangipudy R, Sistare FD, Colman K, Garcia-Tapia D, Monticello T, and Blanset D. Tg.rasH2 mouse model for assessing carcinogenic potential of pharmaceuticals: industry survey of current practices. Int J Toxicol. **39**: 198–206. 2020. [Medline] [CrossRef]
6. Mitsumori K, Koizumi H, Nomura T, and Yamamoto S. Pathological features of spontaneous and induced tumors in transgenic mice carrying a human prototype c-Ha-ras gene used for six-month carcinogenicity studies. Toxicol Pathol. **26**: 520–531. 1998. [Medline] [CrossRef]
7. Kanno H, Tanakamura Z, Ishimura Y, Kandori H, Yamasaki H, and Sasaki S. Historical background data in CB6F1-Tg-rasH2 mice and CB6F1-nonTg-rasH2 mice over a 26-week experimental period. J Toxicol Pathol. **16**: 267–274. 2003. [CrossRef]
8. Long GG, Goodman DG, Credille KM, Mann PC, Wilson JM, and Cardy R. Hematopoietic proliferative lesions in the spleen of rasH2 transgenic mice treated with MNU. Toxicol Pathol. **38**: 1026–1036. 2010. [Medline] [CrossRef]
9. Nambiar PR, Turnquist SE, and Morton D. Spontaneous tumor incidence in rasH2 mice: review of internal data and published literature. Toxicol Pathol. **40**: 614–623. 2012. [Medline] [CrossRef]
10. Paranjpe MG, Elbekaei RH, Shah SA, Hickman M, Wenk ML, and Zahalka EA. Historical control data of spontaneous tumors in transgenic CByB6F1-Tg(HRAS)2Jic (Tg.rasH2) mice. Int J Toxicol. **32**: 48–57. 2013. [Medline] [CrossRef]
11. Paranjpe MG, Denton MD, and Elbekai RH. The 26-week Tg.rasH2 mice carcinogenicity studies: microscopic examination of only select tissues in low- and mid-dose groups. Toxicol Pathol. **42**: 1153–1157. 2014. [Medline] [CrossRef]
12. Paranjpe MG, Belich JL, McKeon ME, Elbekai RH, Mann PC, Hard GC, and Seely JC. Renal tumors in 26-week Tg.rasH2 mice carcinogenicity studies. Toxicol Pathol. **44**:

633–635. 2016. [Medline] [CrossRef]
13. Paranjpe MG, Belich JL, Richardson DR, Vidmar T, Mann PC, McKeon ME, and Elbekai RH. Progression of serosal vascular proliferative lesions to hemangiosarcomas in the uterus of the 26-Week Tg.rasH2 mice carcinogenicity studies. Int J Toxicol. **36**: 29–34. 2017. [Medline] [CrossRef]
14. Paranjpe MG, Belich JL, Mann PC, McKeon ME, Elbekai RH, Brown CM, and Patrick DJ. A comparison of spontaneous tumors in Tg.rasH2 Mice in 26-week carcinogenicity studies conducted at a single test facility during 2004 to 2012 and 2013 to 2018. Toxicol Pathol. **47**: 18–25. 2019. [Medline] [CrossRef]
15. Takaoka M, Sehata S, Maejima T, Imai T, Torii M, Satoh H, Toyosawa K, Tanakamaru ZY, Adachi T, Hisada S, Ueda M, Ogasawara H, Matsumoto M, Kobayashi K, Mutai M, and Usui T. Interlaboratory comparison of short-term carcinogenicity studies using CB6F1-rasH2 transgenic mice. Toxicol Pathol. **31**: 191–199. 2003. [Medline]
16. Paranjpe MG, Shah SA, Denton MD, and Elbekai RH. Incidence of spontaneous non-neoplastic lesions in transgenic CBYB6F1-Tg(HRAS)2Jic mice. Toxicol Pathol. **41**: 1137–1145. 2013. [Medline] [CrossRef]
17. Boyle MH, Paranjpe MG, and Creasy DM. High background incidence of spontaneous subcapsular adrenal gland hyperplasia of Tg.rasH2 mice used in 26-week carcinogenicity studies. Toxicol Pathol. **46**: 444–448. 2018. [Medline] [CrossRef]
18. De Jonghe S, Verbeeck J, Van Deun K, Brown M, Vynckier A, Vandenberghe J, Verstynen B, Lampo A, Monbaliu J, Jansen T, and Coussenent W. Results of 6 month oral carcinogenicity study with 17 beta-estradiol in transgenic TgHrasH2 and wild type mice. In: Workshop on the Evaluation of Alternative Methods for Carcinogenicity Testing. International Life Sciences Institute, Washington DC. 2000.
19. Tsuchiya T, Kobayashi K, Sakairi T, Goto K, Okada M, Sano F, Sugimoto J, Morohashi T, Usui T, and Mutai M. Skeletal myopathy in transgenic mice carrying human prototype c-Ha-ras gene. Toxicol Pathol. **30**: 501–506. 2002. [Medline] [CrossRef]
20. Tamaoki N. The rasH2 transgenic mouse: nature of the model and mechanistic studies on tumorigenesis. Toxicol Pathol. **29**(Suppl): 81–89. 2001. [Medline] [CrossRef]
21. Frith CH, Highman B, Burger G, and Sheldon WD. Spontaneous lesions in virgin and retired breeder BALB/c and C57BL/6 mice. Lab Anim Sci. **33**: 273–286. 1983. [Medline]
22. Frith CH, Ward JM. Color Atlas of Neoplastic and Nonneoplastic Lesions in Aging Mice. CL Davis DVM foundation, Gurnee. 1988.
23. Pettan-Brewer C, and Treuting PM. Practical pathology of aging mice. Pathobiol Aging Age Relat Dis. **1**: 7202. 2011. [Medline] [CrossRef]
24. Cora MC, Kooistra L, and Travlos G. Vaginal cytology of the laboratory rat and mouse: review and criteria for the staging of the estrous cycle using stained vaginal smears. Toxicol Pathol. **43**: 776–793. 2015. [Medline] [CrossRef]
25. Cooper TK, Meyerholz DK, Beck AP, Delaney MA, Piersigilli A, Southard TL, and Brayton CF. Research-relevant conditions and pathology of laboratory mice, rats, gerbils, guinea pigs, hamsters, nake mode rats, and rabbits. ILAR J. **62**: 77–132. 2021. [Medline] [CrossRef]
26. Pearse G. Histopathology of the thymus. Toxicol Pathol. **34**: 515–547. 2006. [Medline] [CrossRef]
27. Doi T, Kotani Y, Kokoshima H, Kanno T, Wako Y, and Tsuchitani M. Eosinophilic substance is “not amyloid” in the mouse nasal septum. Vet Pathol. **44**: 796–802. 2007. [Medline] [CrossRef]
28. Monticello TM, Morgan KT, and Uraih L. Nonneoplastic nasal lesions in rats and mice. Environ Health Perspect. **85**: 249–274. 1990. [Medline]
29. Chamanza R, and Wright JA. A review of the comparative anatomy, histology, physiology and pathology of the nasal cavity in rats, mice, dogs and non-human primates. Relevance to inhalation toxicity and human health risk assessment. J Comp Pathol. **153**: 287–314. 2015. [Medline] [CrossRef]

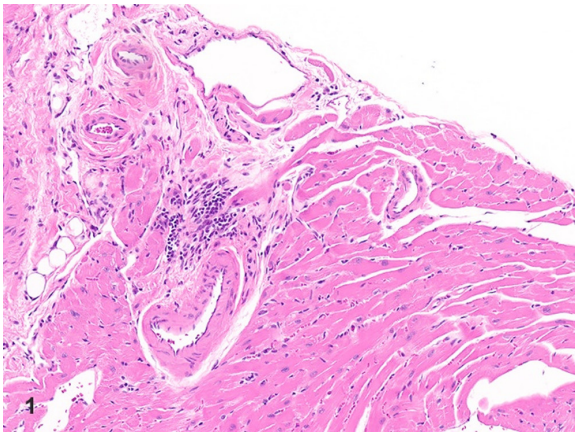


**Fig. 1.** Heart: Mononuclear cell infiltrate. Mononuclear cell infiltrates, primarily lymphocytes and macrophages, are occasionally noted in the atria and/or ventricles without any associated degenerative changes.

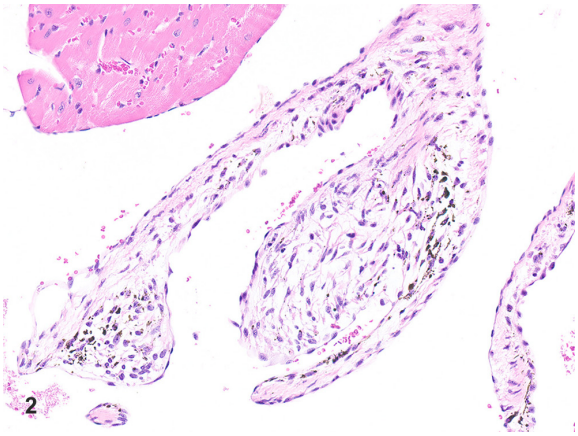


**Fig. 2.** Heart: Pigment, valve. Black pigment in the interstitium of the heart valves is a common finding.

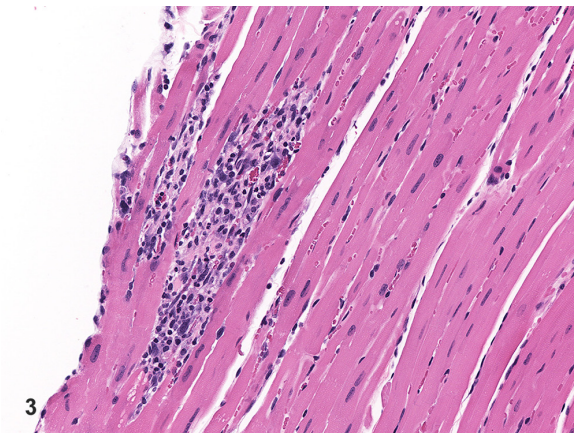


**Fig. 3.** Heart: Mixed cell inflammation and cardiomyocyte degeneration/necrosis. Mixed cell inflammation associated with cardiomyocyte degeneration and necrosis sporadically occurs in the atria or ventricles (rodent cardiomyopathy).

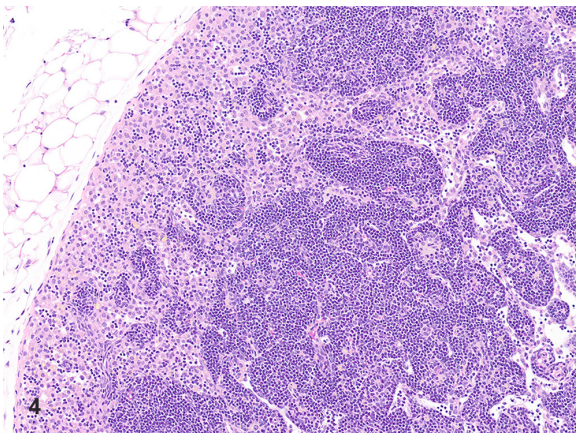


**Fig. 4.** Mesenteric Lymph Node: Increased sinus macrophages. Increased numbers of macrophages within the lymph node sinuses are occasionally observed.

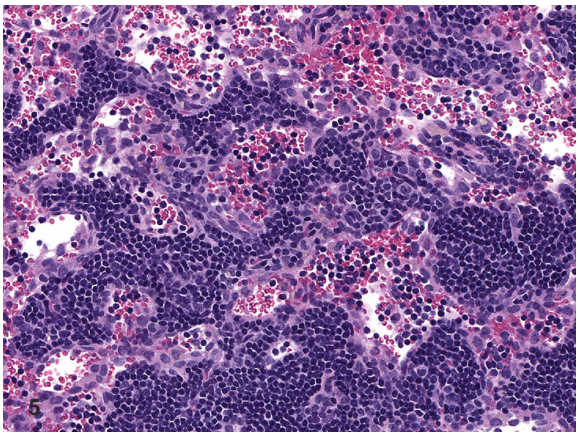


**Fig. 5.** Mesenteric lymph node: Increased sinus erythrocytes. Sinuses (subcapsular and/or medullary) of lymph nodes are filled with erythrocytes.

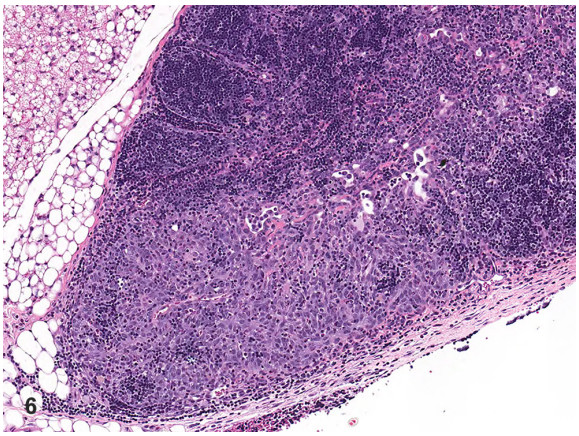


**Fig. 6.** Thymus: Epithelial hyperplasia. Proliferation of spindled epithelial cells is occasionally observed in the thymus.

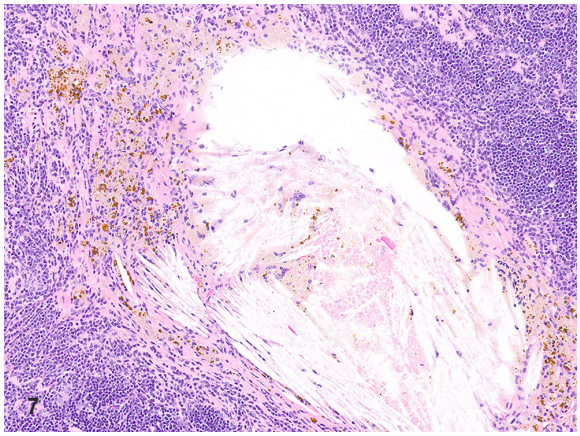

**Fig. 7.** Thymus: Cholesterol granuloma. A focus of clear, acicular clefts associated with brown (hemosiderin) and yellow (hematoidin) pigment is bounded by macrophages.

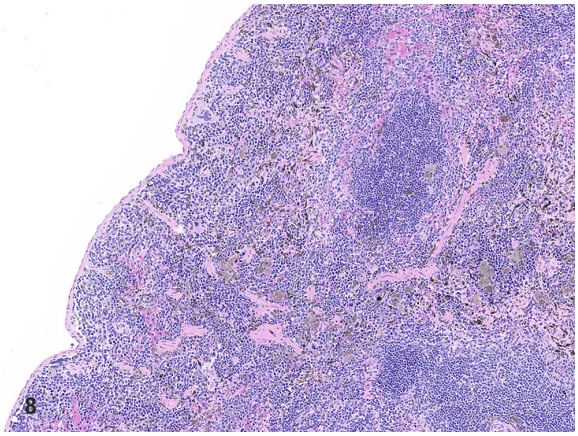

**Fig. 8.** Spleen: Pigment. Pigment, often noted in the red pulp, is a common finding and is sometimes observed macroscopically as focal red or black discoloration.

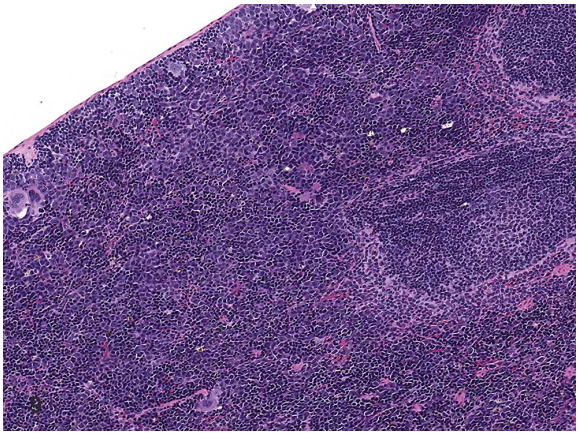

**Fig. 9.** Spleen: Extramedullary hematopoiesis. Increased progenitor hematopoietic cells (erythroid and myeloid) are noted in the red pulp. This finding is most profound in conditions resulting in physiologic hematopoiesis, such as inflammation, blood loss, neoplasia (e.g. hemangiosarcoma), etc.

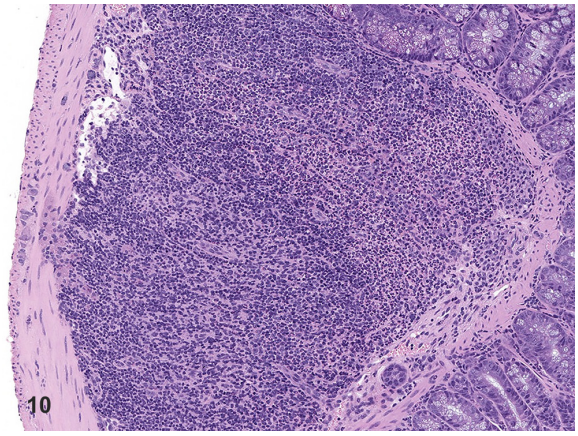

**Fig. 10.** GALT/Peyer's Patch: Neutrophil infiltrate. Neutrophilic infiltrates are sometimes noted in the gut-associated lymphoid tissue (GALT) without any associated degenerative changes.

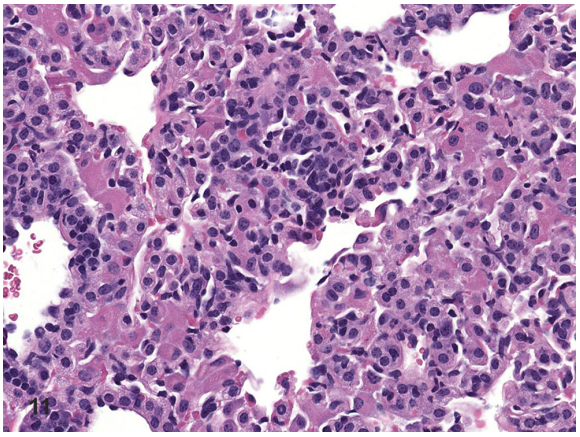

**Fig. 11.** Lung: Alveolar macrophage accumulation and mononuclear cell infiltrate. Accumulation of macrophages in alveoli and adjacent bronchioles.

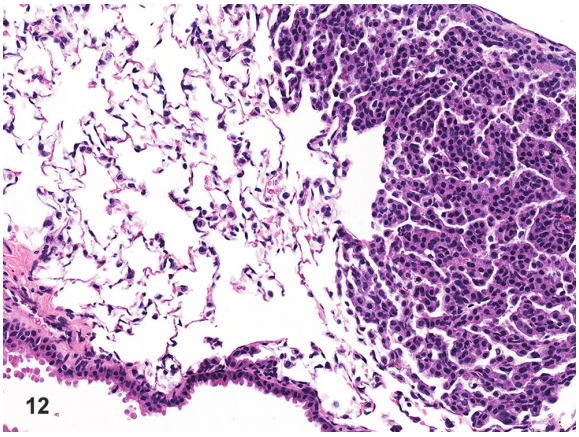

**Fig. 12.** Lung: Bronchiolo-alveolar hyperplasia. Focal proliferation of bronchiolo-alveolar epithelial cells, sometimes associated with inflammatory cells and/or foreign material, is relatively common in the lung.

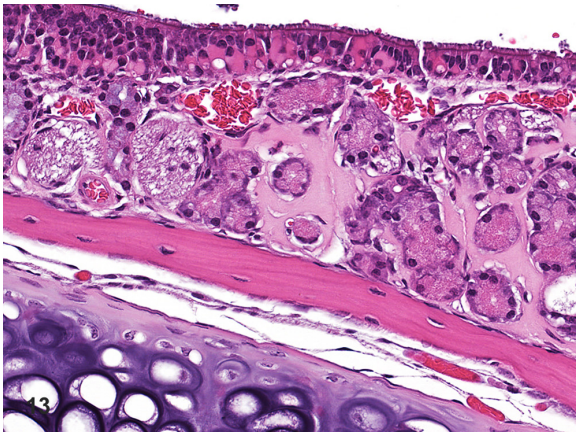


**Fig. 13.** Nasal Turbinates: Eosinophilic globules and amyloid-like material, septum. Cytoplasmic, hyalinized inclusions in the respiratory epithelium and amyloid-like deposits in the interstitium surrounding seromucous glands occur in the ventral nasal septum, particularly in males.

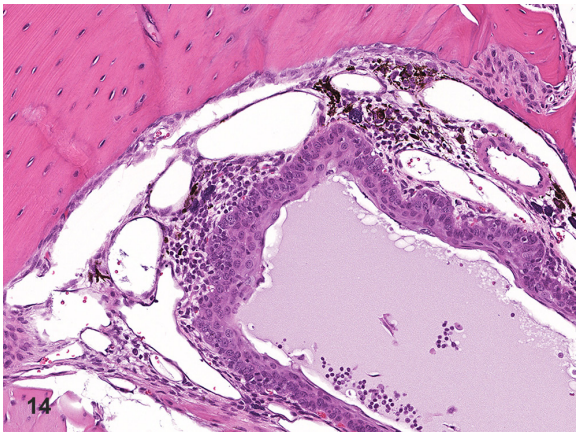


**Fig. 14.** Nasal Turbinates: Pigment, paranasal sinus. Pigment in the subepithelial interstitium is a common finding in the paranasal sinus of both sexes.

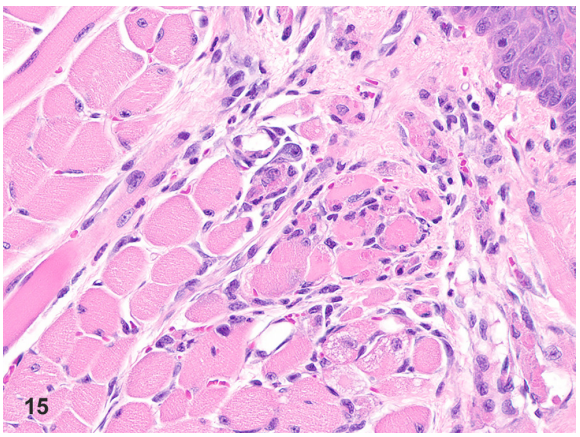


**Fig. 15.** Tongue: Muscle degeneration/regeneration. Myocyte degeneration and regeneration is occasionally noted in muscle of the tongue.

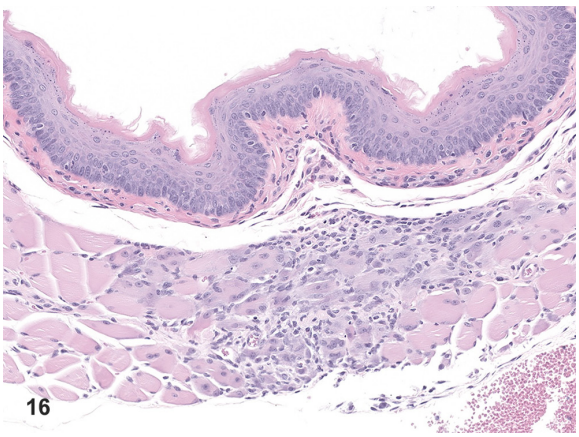


**Fig. 16.** Esophagus: Muscle degeneration/regeneration. Myocyte degeneration and regeneration is sometimes noted as a spontaneous finding in the muscle of the esophagus.

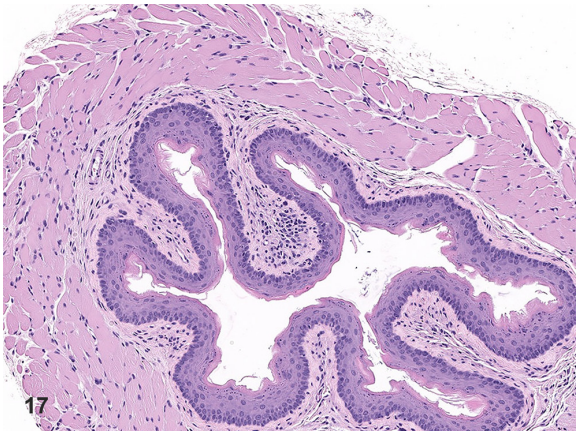


**Fig. 17.** Esophagus: Mononuclear cell infiltrate. Mononuclear inflammatory cell infiltrates, primarily lymphocytes and macrophages, are occasionally noted in the lamina propria/submucosa.

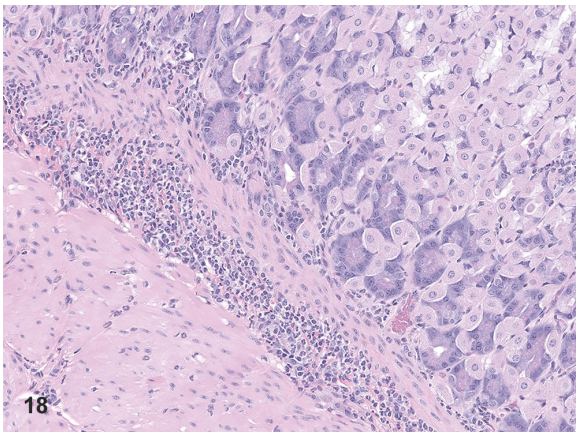


**Fig. 18.** Stomach, Glandular: Neutrophil infiltrate. Neutrophilic infiltrates, without any associated degenerative changes, are occasionally noted in the lamina propria and/or submucosa of the glandular stomach, more often at limiting ridge and with hyperplasia of overlying epithelium.

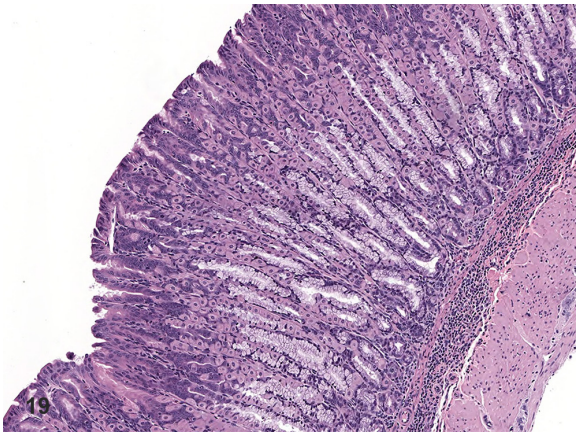


**Fig. 19.** Stomach, Glandular: Mixed cell infiltrate. Mixed inflammatory cells infiltrate the lamina propria and submucosa.

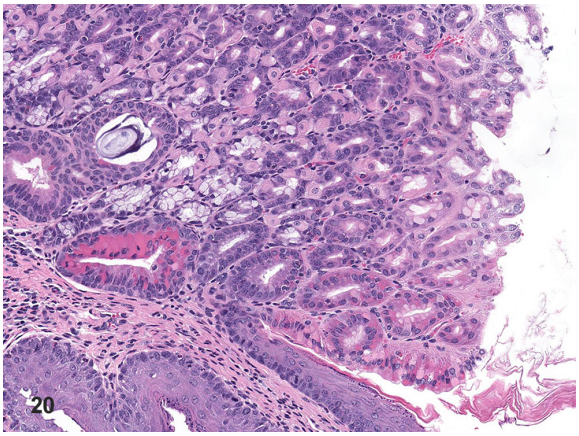


**Fig. 20.** Glandular stomach: Eosinophilic globules and mixed cell infiltrate. Mucus neck cells near the limiting ridge are distended by bright, hyalinized, eosinophilic cytoplasm, with an adjacent mixed cell infiltrate and ectatic glands containing mucus.

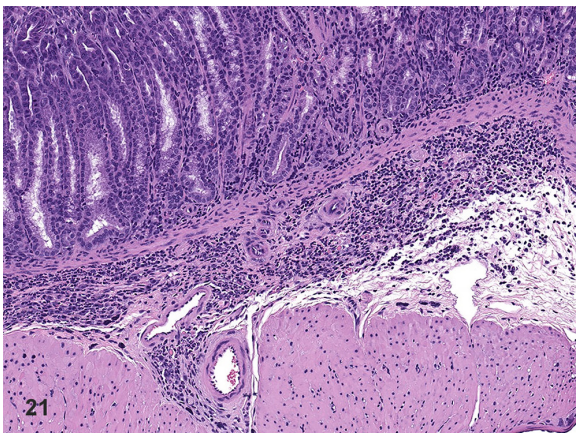


**Fig. 21.** Stomach, Glandular: Mixed cell inflammation. Mixed inflammatory cells associated with cellular debris disrupt the architecture of the submucosa and lamina propria.

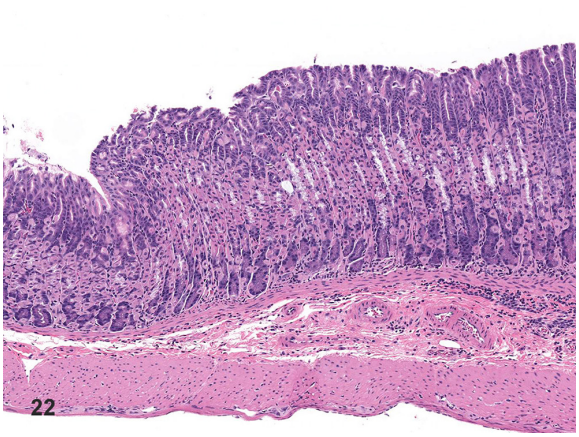


**Fig. 22.** Glandular stomach: Hyperplasia, mucosa: Thickened glandular mucosa, increased epithelial basophilia, and elongation of gastric crypts characterize the early features of this sporadic finding.

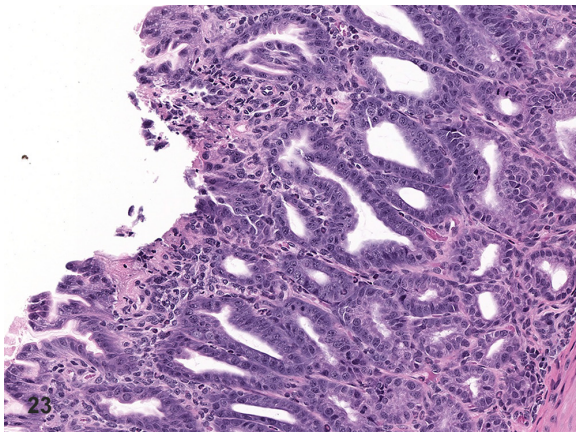


**Fig. 23.** Stomach, glandular: Erosion: There is focally extensive loss of the superficial mucosa associated with mixed inflammation and cellular debris, consistent with erosion. Because the plane of section may impact the microscopic depth of the finding in the mucosa, the term erosion/ulcer is often applied.

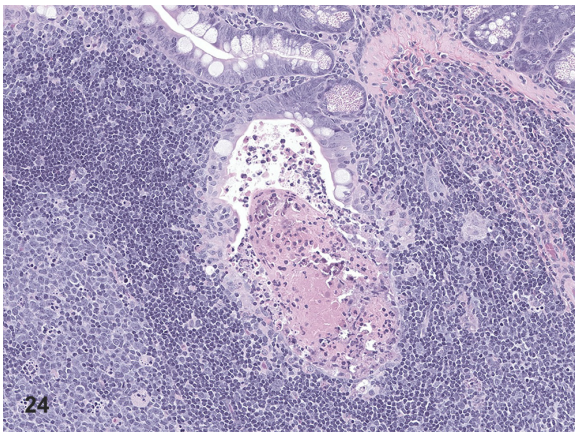


**Fig. 24.** Small Intestine, Ileum: Neutrophil infiltrate and crypt dilatation. Neutrophils infiltrate the lamina propria and mucosa and extend into a dilated crypt adjacent to the underlying GALT/PP in this occasional finding.

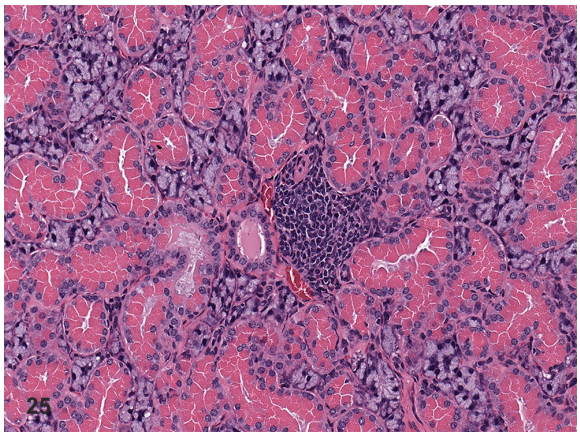


**Fig. 25.** Salivary Gland, Submandibular: Mononuclear cell infiltrate. Mononuclear cells infiltrate the connective tissue surrounding acini and a duct. This is a common finding.

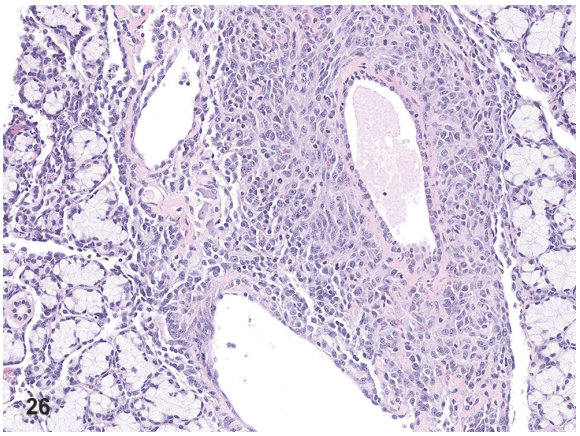


**Fig. 26.** Salivary Gland, Sublingual: Mixed cell infiltrate. Mixed inflammatory cells infiltrate the connective tissue surrounding a dilated duct and adjacent acini is an occasional finding.

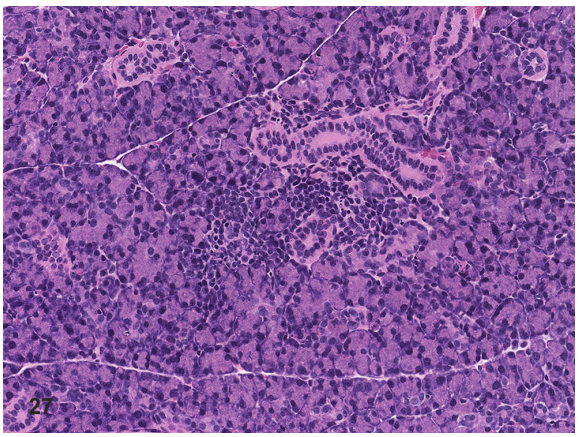


**Fig. 27.** Salivary Gland, Parotid: Mononuclear cell infiltrate. Infiltrates of mononuclear inflammatory cells are common in the salivary glands, including the parotid, and often occur around ducts.

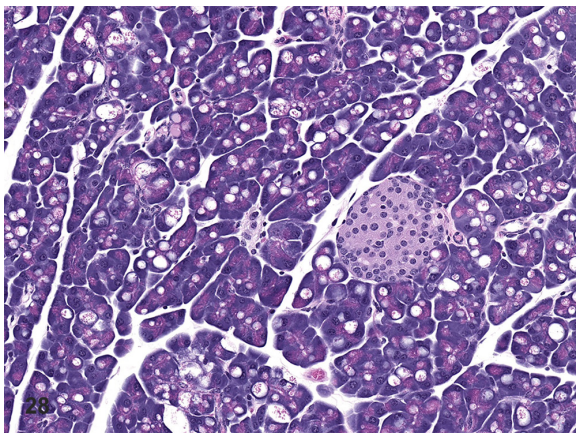


**Fig. 28.** Pancreas: Acinar cell vacuolation. A single large or multiple few, discrete, clear cytoplasmic vacuoles occasionally displace nuclei of exocrine acinar cells. This is an occasional finding in the pancreas.

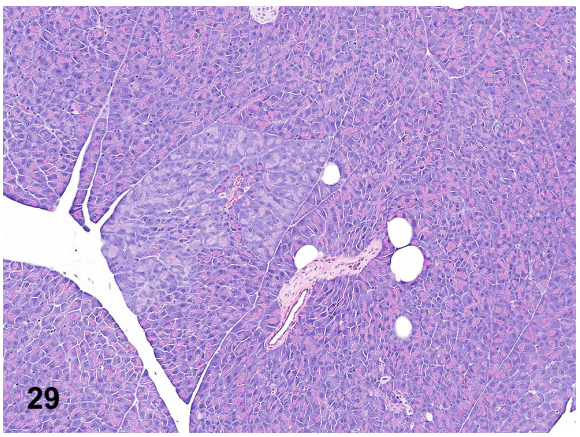


**Fig. 29.** Pancreas: Focus of cellular alteration, basophilic. A focus of tinctorially distinct (basophilic), small acini with no compression of adjacent parenchyma is an infrequent background finding.

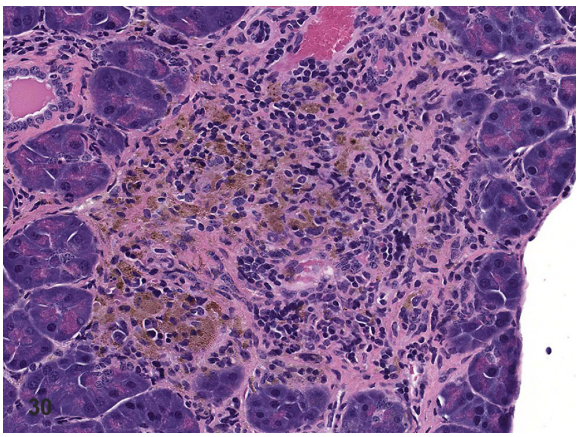


**Fig. 30.** Pancreas: Fibrosis, mixed cell infiltrate and pigment. Fibrosis and mixed inflammatory cell infiltrates occasionally occur in the pancreas; in this case there is also accompanying pigment.

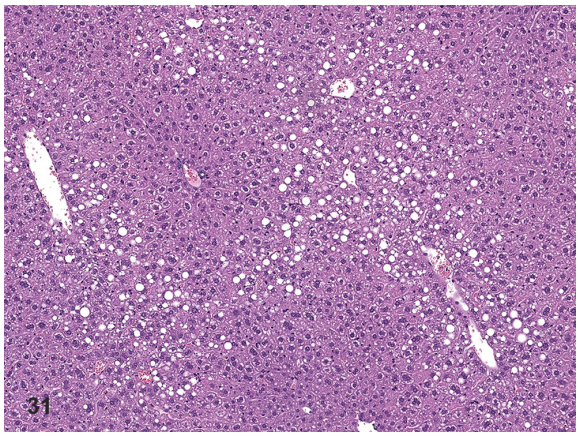


**Fig. 31.** Liver: Hepatocyte vacuolation. Single, large or few small clear, discrete cytoplasmic vacuoles are occasional finding in the liver.

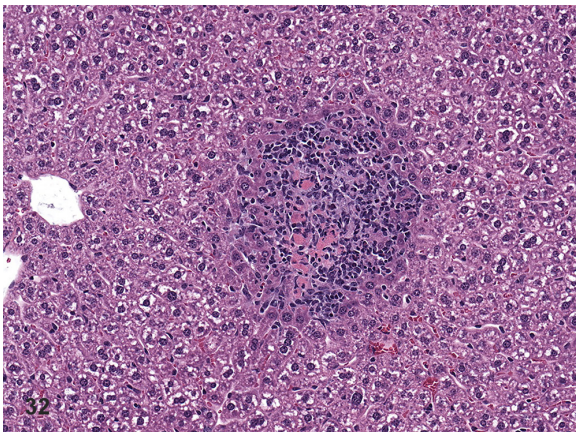


**Fig. 32.** Liver: Mixed cell infiltrate. Mixed inflammatory cells focally infiltrate hepatic cords. Random infiltrates of mixed and mononuclear inflammatory cells are common in the liver.

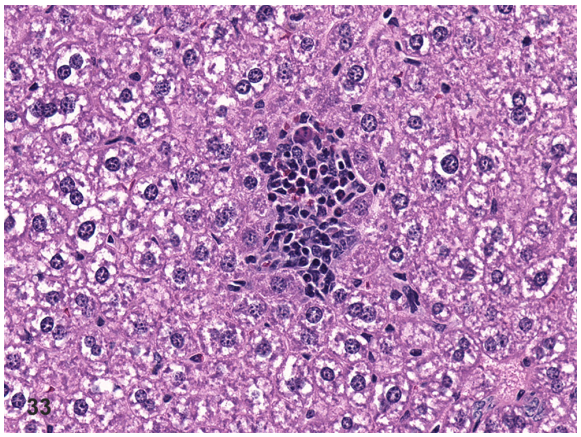


**Fig. 33.** Liver: Extramedullary hematopoiesis. A small focus of hematopoietic progenitor cells is noted within hepatic sinusoids. This occasional finding in the liver, often concurrently with the same finding in the spleen, is frequently due to secondary physiologic responses associated with inflammation, blood loss, neoplasia (e.g. hemangiosarcoma), etc.

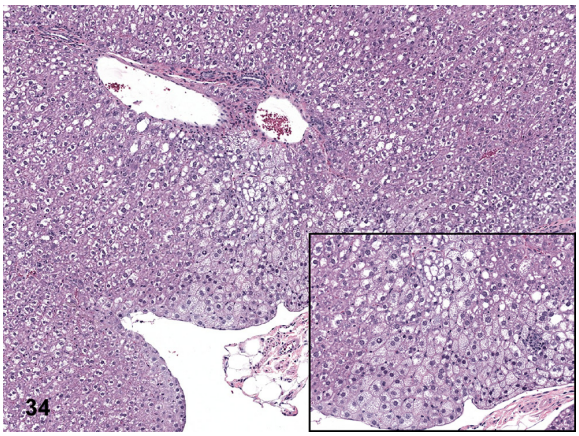


**Fig. 34.** Liver: Tension lipidosis. Focal cytoplasmic vacuolation of subcapsular hepatocytes is occasionally noted in the liver, particularly near the gall bladder. Inset: higher magnification.

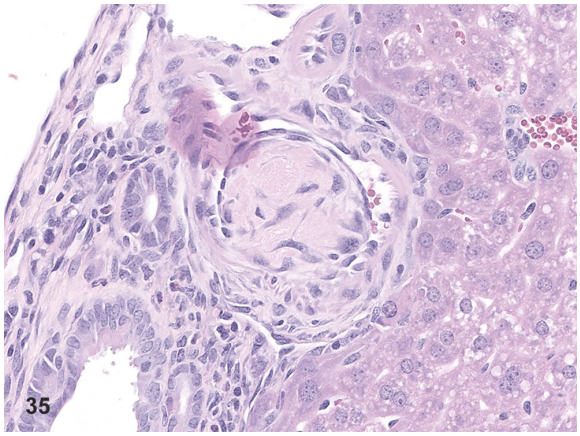


**Fig. 35.** Liver: Thrombus. A thrombus partially occludes a portal vessel and is lined by endothelial cells (recanalization).

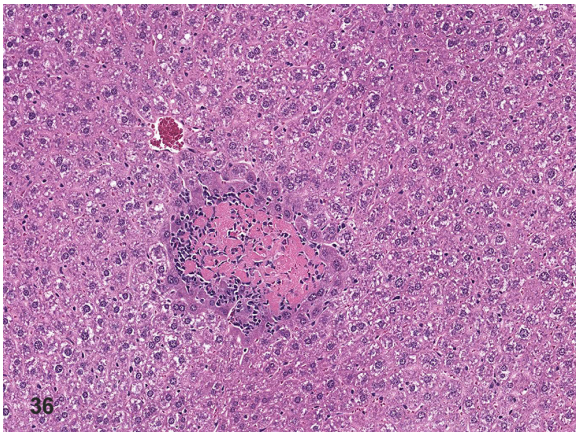


**Fig. 36.** Liver: Focal necrosis and mononuclear cell infiltrate. Focal hypereosinophilia with loss of hepatic cord architecture and cellular detail, sometimes rimmed by few mononuclear or mixed inflammatory cells, characterizes this occasional finding.

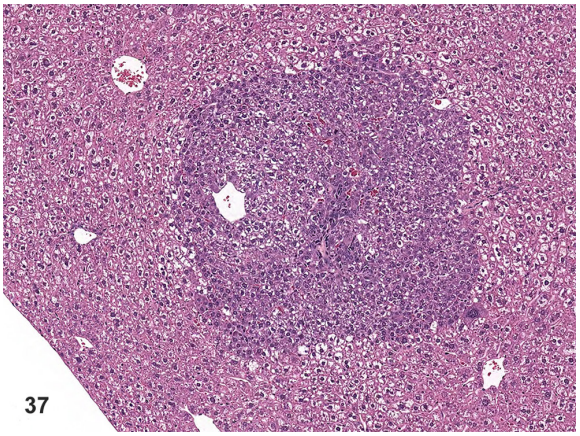


**Fig. 37.** Liver: Focus of cellular alteration, basophilic. A well-circumscribed focus of tinctorially distinct (basophilic), small hepatocytes that merge with adjacent hepatic cords with little compression of adjacent parenchyma is an infrequent background finding.

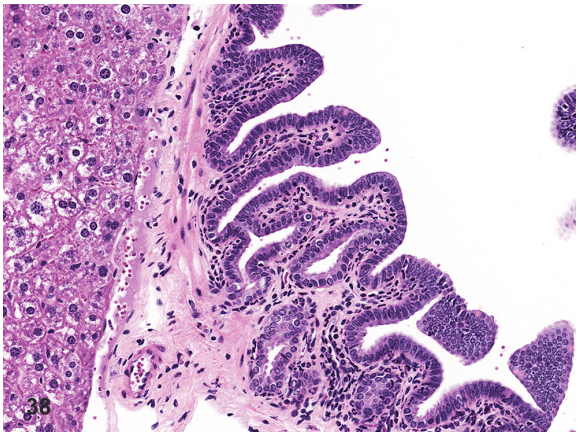


**Fig. 38.** Gall Bladder: Mixed cell infiltrate. Mixed inflammatory cell infiltrates are sometimes noted in the gall bladder subepithelial connective tissue.

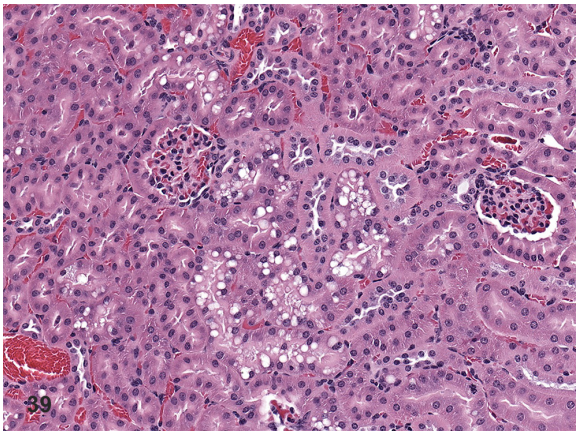


**Fig. 39.** Kidney: Tubule vacuolation, cortex. Cortical tubule epithelial cells contain clear, discrete, cytoplasmic vacuoles in this occasional finding in the kidney cortex.

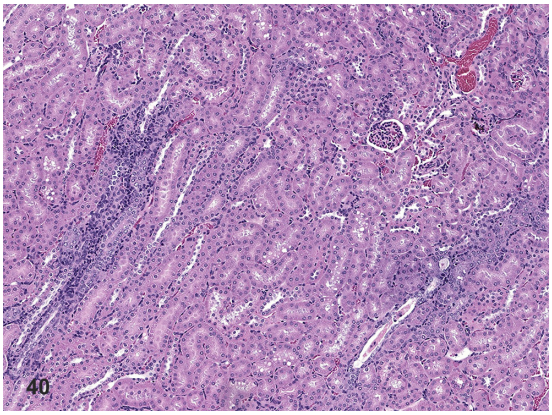


**Fig. 40.** Kidney: Chronic progressive nephropathy. Basophilic tubules, interstitial mononuclear cell infiltrates, and few hyaline casts (not shown) occasionally occur in the kidney cortex.

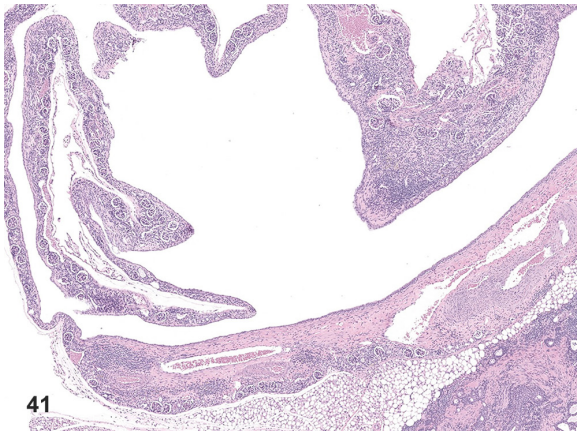


**Fig. 41.** Kidney: Cyst. A large, empty, epithelial lined cyst compresses the adjacent atrophied cortex in this occasional finding.

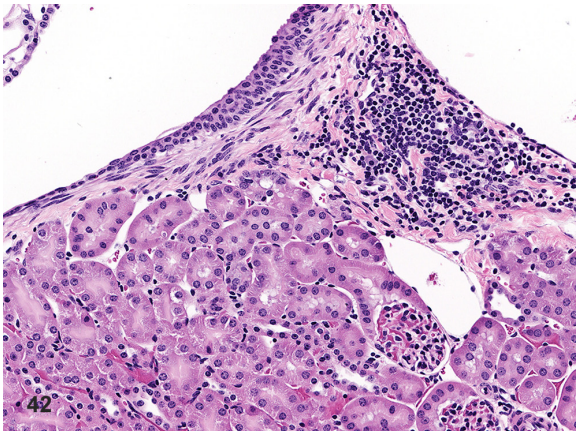


**Fig. 42.** Kidney: Mononuclear cell infiltrate. Mononuclear cell infiltrates are common in the kidney, particularly in the vicinity of the pelvis.

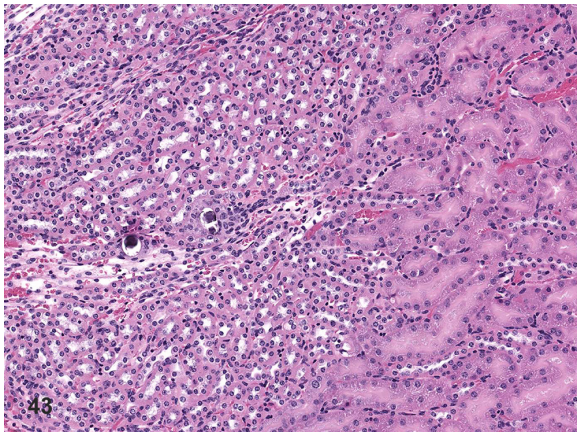


**Fig. 43.** Kidney: Tubule mineralization. Scattered individual tubule mineralization, primarily near the corticomedullary junction, is not uncommon, particularly in females.

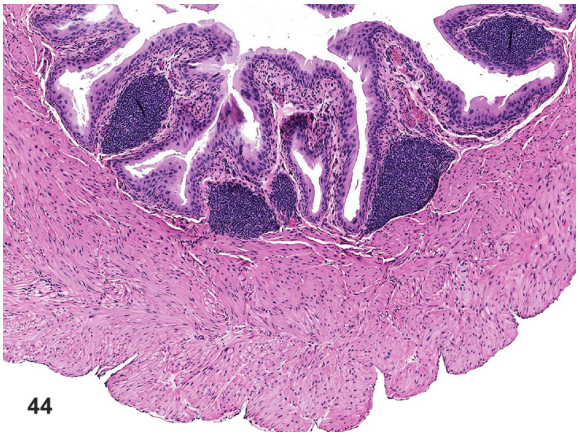


**Fig. 44.** Urinary Bladder: Mononuclear cell infiltrate. Mononuclear cell infiltrates are common in the lamina propria/submucosa of the urinary bladder.

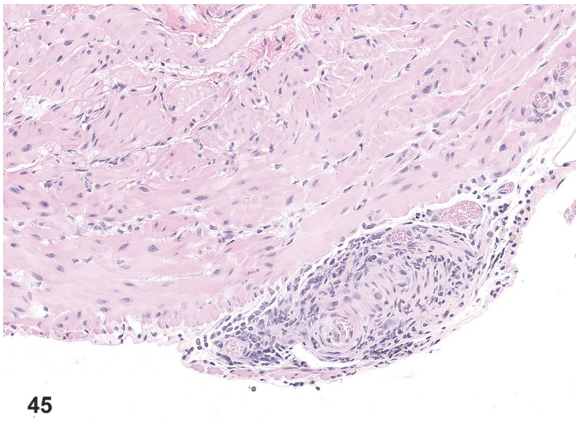


**Fig. 45.** Urinary Bladder: Vessel inflammation, mixed cell. Mixed inflammatory cells infiltrate and expand the wall of a vessel on the serosa of the urinary bladder in this infrequent finding that in various tissues

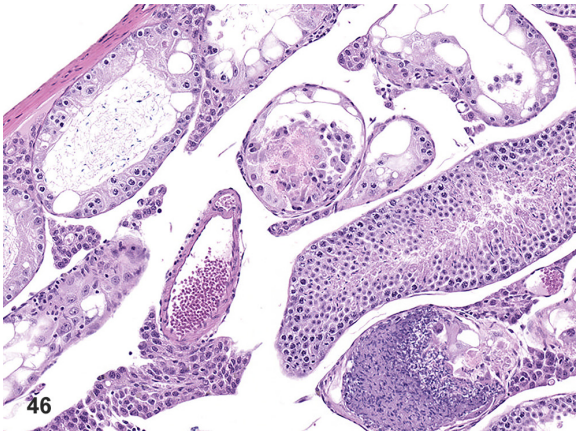


**Fig. 46.** Testis: Seminiferous tubule degeneration/atrophy and sperm granuloma. Tubules devoid of germ cells and lined by Sertoli cells only or contain multinucleated germ cells admixed with multinucleated macrophages and cell debris is noted as occasional finding.

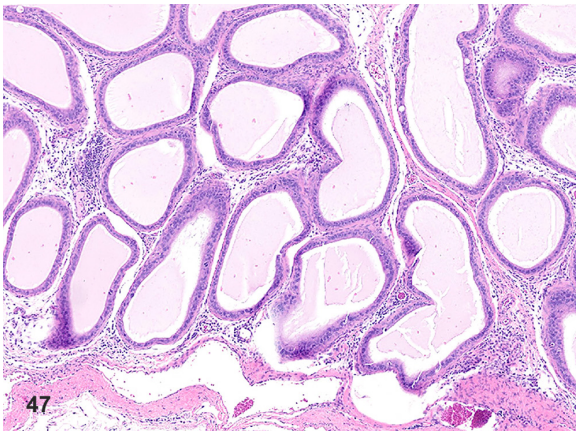


**Fig. 47.** Epididymis: Mononuclear cell infiltrate and reduced sperm. Mononuclear cells infiltrate the connective tissue surrounding ducts, and tubule lumina are devoid of sperm and contain only proteinaceous fluid.

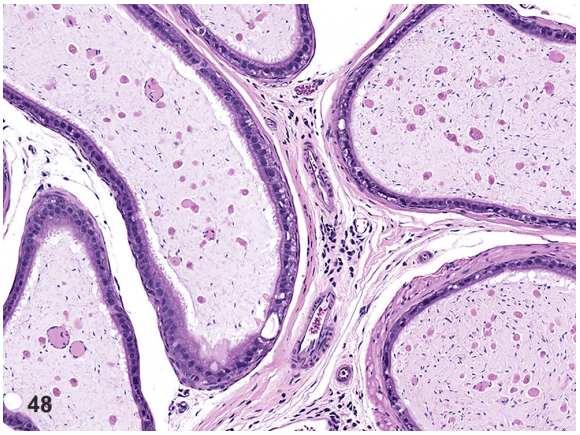


**Fig. 48.** Epididymis: Cell debris. Ducts contain amorphous cell debris and proteinaceous fluid with few sperm.

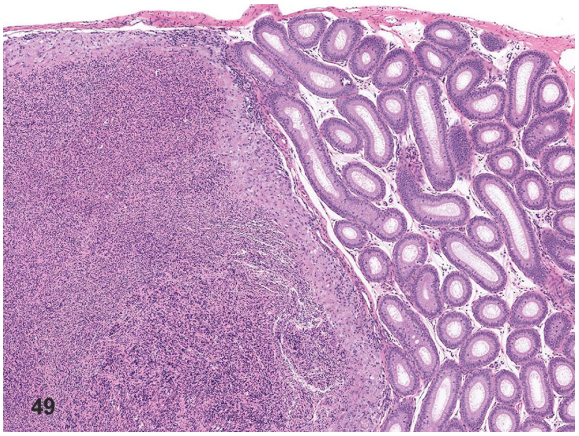


**Fig. 49.** Epididymis: Sperm granuloma. Large, epithelioid macrophages expand the connective tissue surrounding a markedly dilated duct filled with sperm and cellular debris in this sporadic finding.

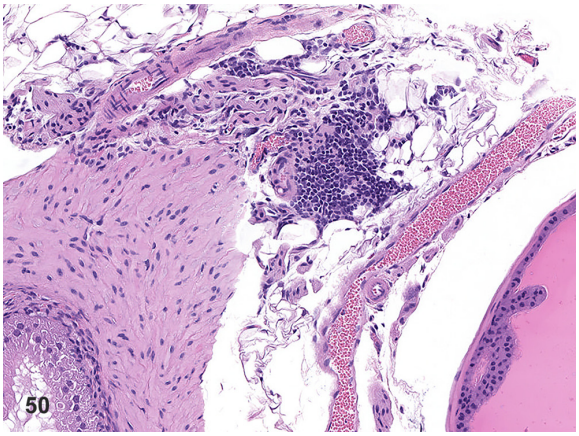


**Fig. 50.** Prostate: Mononuclear cell infiltrate. Mononuclear cells infiltrate within the intertisitum of the connective tissue supporting glands is a common finding.

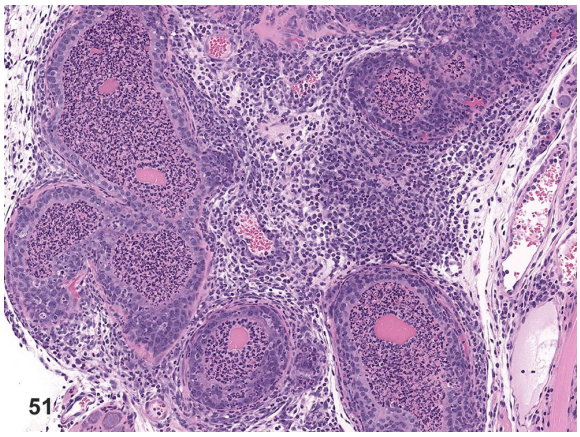


**Fig. 51.** Prostate: Mixed cell inflammation. Numerous mixed inflammatory cells, with a prominent neutrophilic component, infiltrate and expand the interstitium and disrupt and replace acini that are lined by degenerate epithelial cells in this occasional finding.

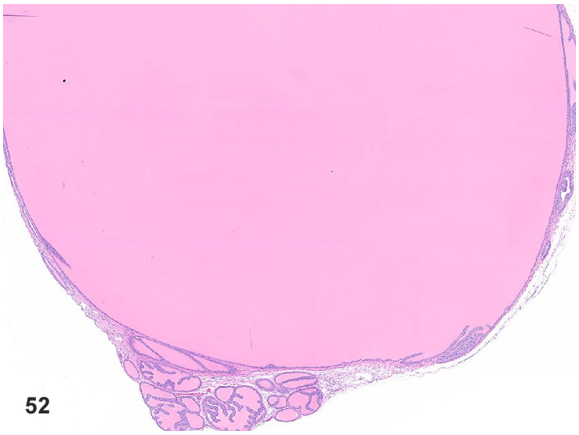


**Fig. 52.** Coagulating Gland: Acinar dilation/increased secretion. A dilated glandular acinus with increased secretory product compresses adjacent acini in this common finding.

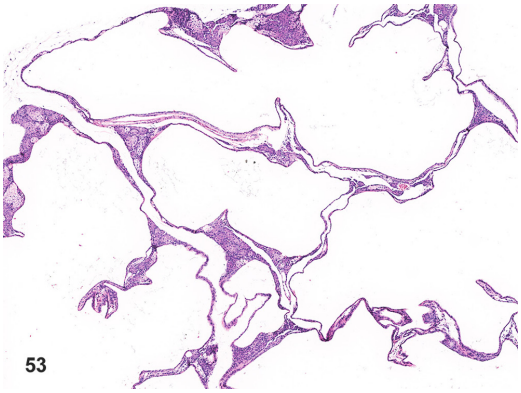


**Fig. 53.** Preputial Gland: Duct dilation. Markedly expanded ducts compress adjacent sebaceous acini in this common finding in males.

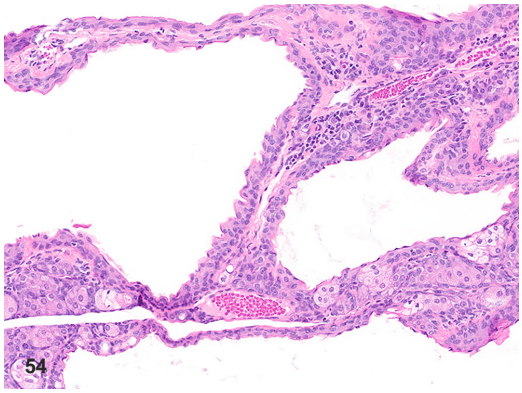


**Fig. 54.** Preputial Gland: Mononuclear cell infiltrate and duct dilation. Mononuclear cells infiltrate the connective tissue surrounding dilated ducts in these common findings in males.

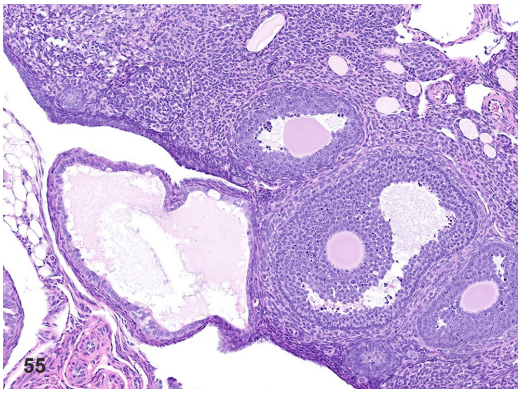


**Fig. 55.** Ovary: Cyst. A small cyst lined by cuboidal epithelial cells is noted within the cortex in this occasional finding in the ovarian cortex, differentiated from a post-ovulatory follicle by its location and lack of granulosa cells.

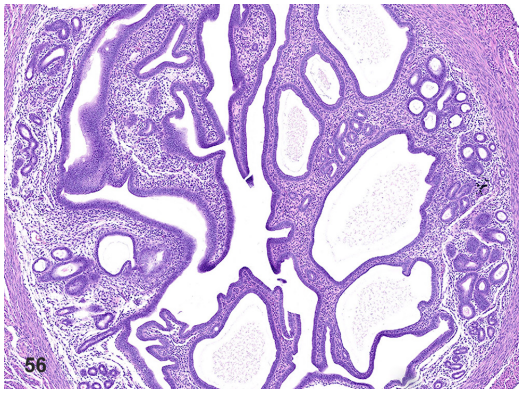


**Fig. 56.** Uterus: Cystic endometrial hyperplasia. Hyperplasia and dilation of uterine glands is a common finding.

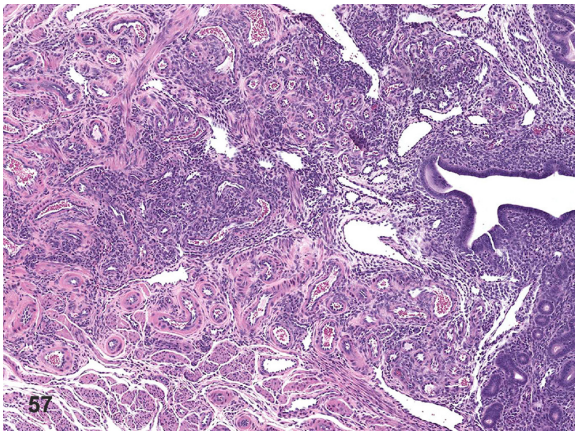


**Fig. 57.** Uterus: Vascular anomaly. This sporadic finding, most often in the uterus and urinary bladder of females, and less often in other tissues of males, is typified by clusters of thick-walled vessels filled with blood and lined by well-differentiated endothelium. These are reportedly progress to vascular neoplasia.

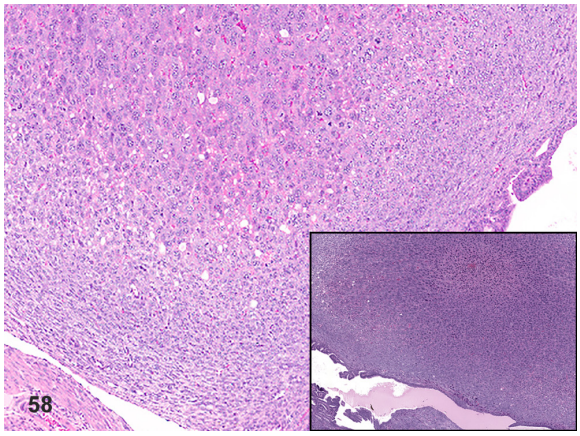


**Fig. 58.** Uterus: Decidual reaction. A nodular proliferation of large, eosinophilic, stromal cells expanding the uterine submucosa is an infrequent finding. Insert: lower magnification.

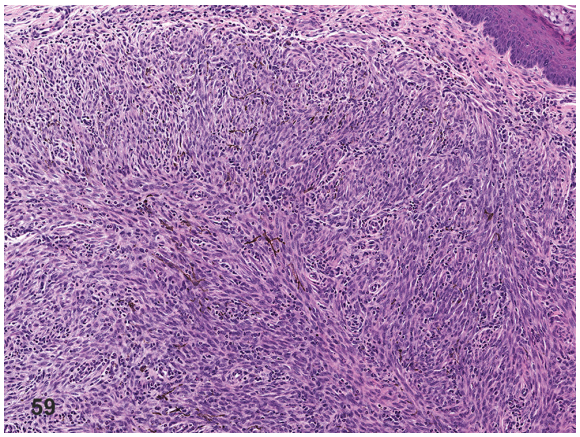


**Fig. 59.** Cervix: Pigment. Pigment is sporadically noted in the female reproductive tissues, particularly in the wall of the uterus, cervix, and vagina.

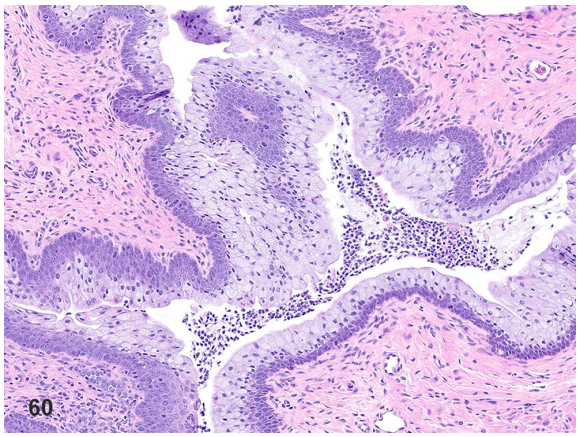


**Fig. 60.** Vagina: Neutrophil infiltrate and increased mucification. Neutrophil (and mixed cell) infiltrates are common in the vagina, typified by inflammatory cells that transmigrate the mucosa and accumulate in the lumen; in this case, there is also increased vacuolation of the epithelium (mucification).

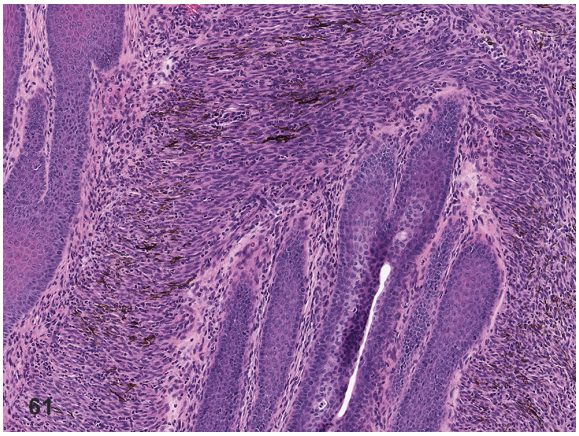


**Fig. 61.** Vagina: Pigment. Pigment is sporadically noted in the female reproductive tissues, particularly in the wall of the uterus, cervix, and vagina.

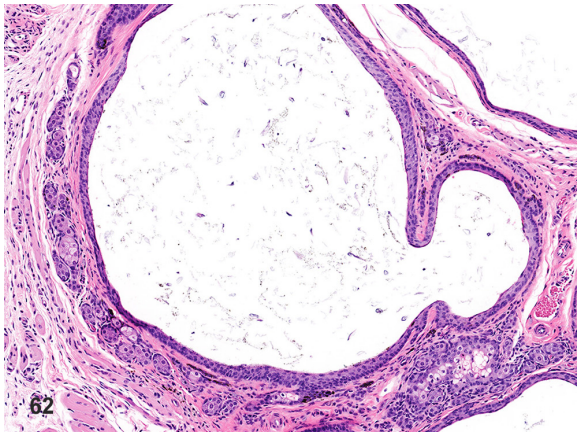


**Fig. 62.** Clitoral Gland: Duct dilation and mononuclear cell infiltrate. Common in females, enlarged ducts filled with secretory material and lined by attenuated epithelium compress adjacent sebaceous acini.

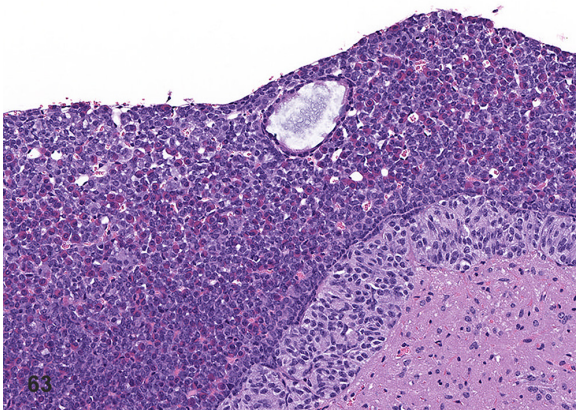


**Fig. 63.** Pituitary: Cyst. A small epithelial lined cyst is noted in the pars distalis in this common finding of the pituitary.

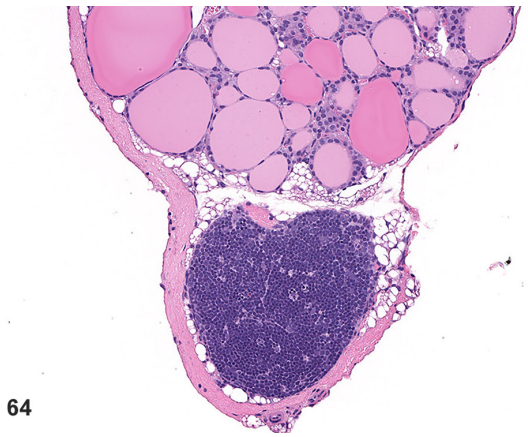


**Fig. 64.** Thyroid: Ectopic thymus tissue. Ectopic thymus tissue occasionally occurs in the thyroid and parathyroid because they each derive from the primordium in the pharyngeal cavity.

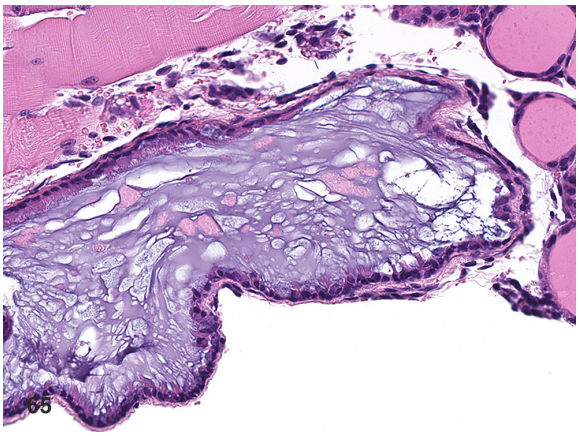


**Fig. 65.** Thyroid: Cyst. A cyst containing amphophilic proteinaceous material and lined by ciliated cuboidal epithelium is noted in this common finding of the thyroid.

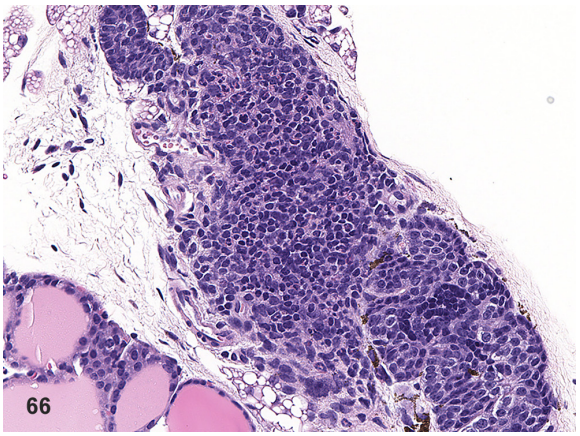


**Fig. 66.** Parathyroid: Mixed cell infiltrate. Mixed and mononuclear cell infiltrates within the interstitium of the parathyroid gland occur sporadically in both sexes.

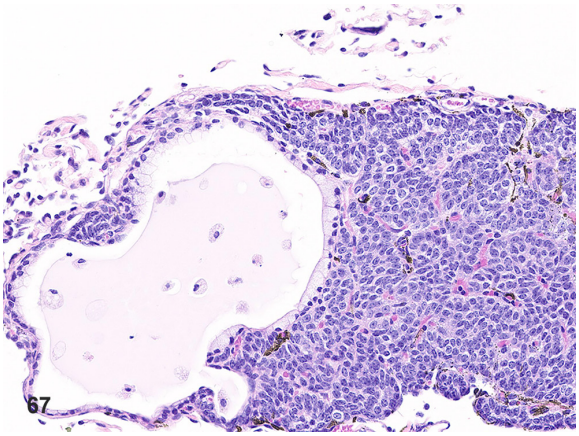


**Fig. 67.** Parathyroid: Cyst and pigment. A cyst containing pale eosinophilic material and few macrophages and lined by cuboidal epithelium occurs in the parathyroid; scattered pigment is noted in the adjacent connective tissue. Both are common findings in the parathyroid.

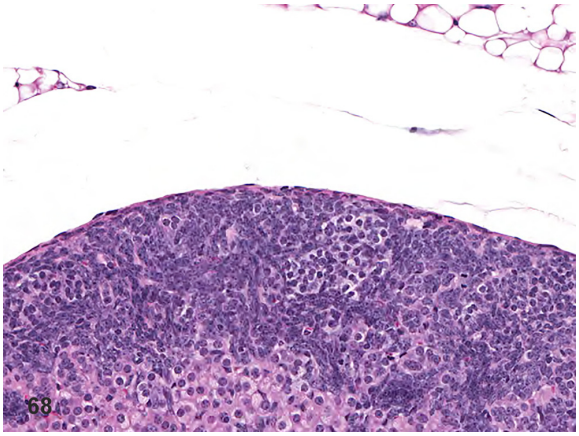


**Fig. 68.** Adrenal Cortex: Subcapsular cell hyperplasia. Hyperplastic basophilic fusiform cells extending from the subcapsular regions into the deeper levels of the zona fasciculata characterizes common finding, particularly in females.

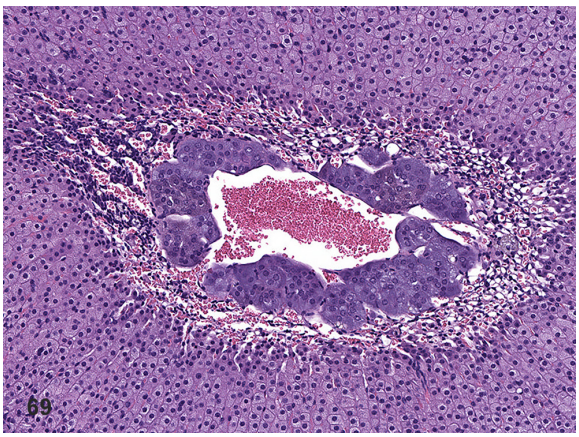


**Fig. 69.** Adrenal Cortex: X-zone degeneration. A rim of hypertrophied and fused vacuolated cortical cells is observed in the deep layers of the zona fasciculata at the corticomedullary junction, and most often noted in females.

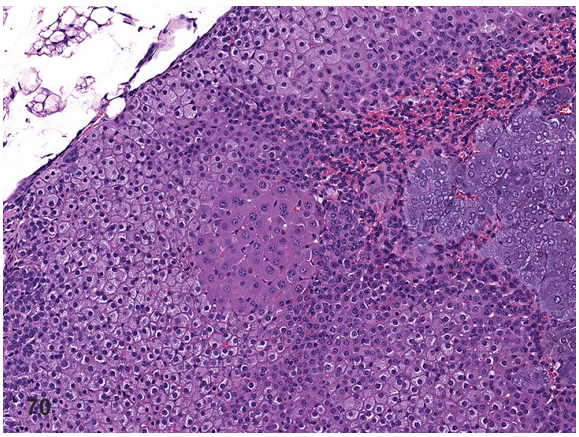


**Fig. 70.** Adrenal Cortex: Focal cortical hypertrophy/hyperplasia. A discrete focus of enlarged, eosinophilic, polygonal cells is observed within the zona fasciculata in this occasional finding.

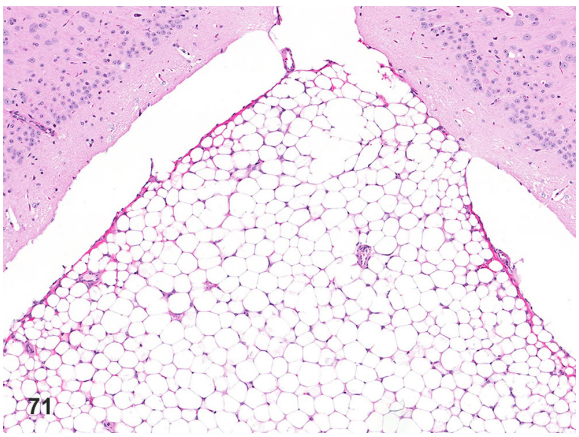


**Fig. 71.** Brain: Lipomatous hamartoma. A non-neoplastic space occupying mass composed of mature, well-differentiated adipocytes that partially fills the ventricle characterizes this uncommon spontaneous finding.

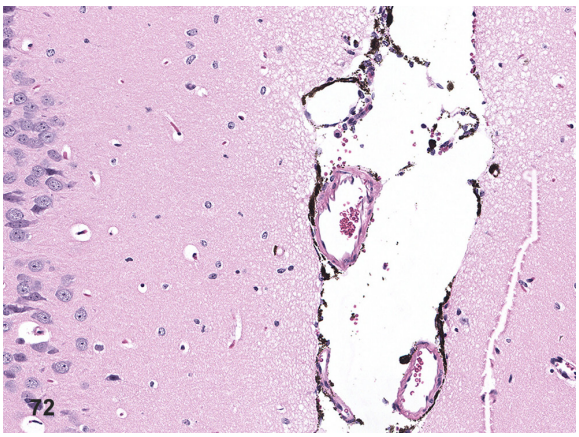


**Fig. 72.** Brain: Pigment, meninges. Pigment in the meninges of the brain, among other tissues, is common.

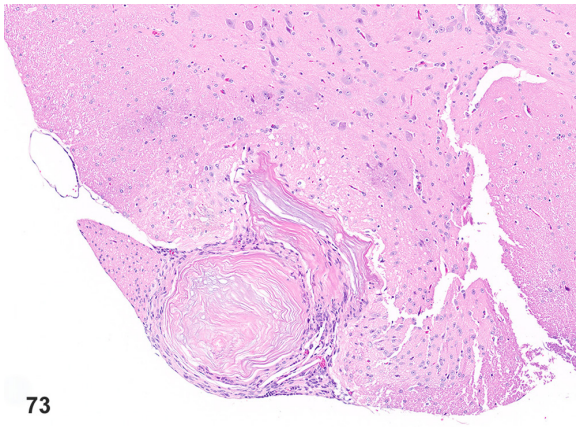


**Fig. 73.** Spinal Cord: Squamous cyst. A cyst lined by keratinizing squamous epithelium filled with concentric layers of keratin that focally expands the meninges and compresses the adjacent gray and white matter typify this infrequent finding.

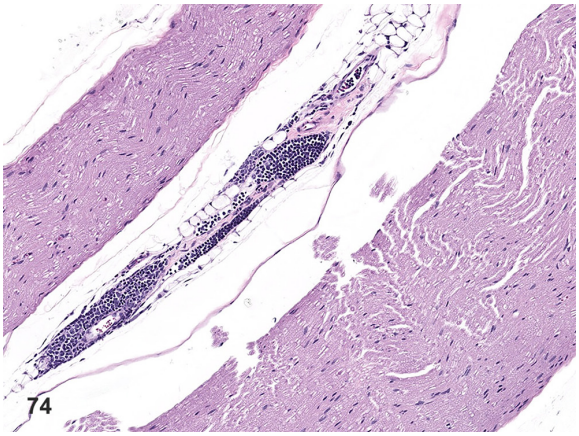


**Fig. 74.** Sciatic Nerve: Mononuclear cell infiltrate. A focal aggregate of mononuclear inflammatory cells infiltrates.

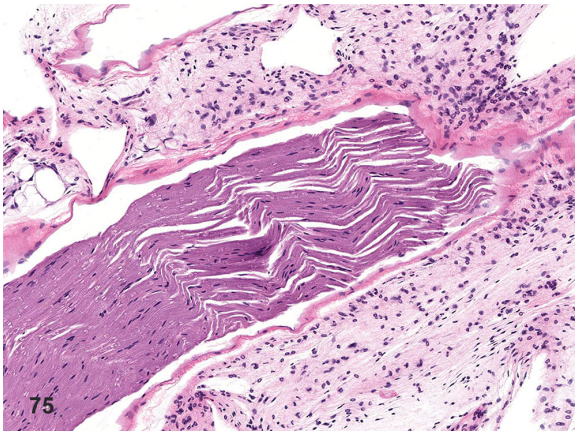


**Fig. 75.** Sciatic Nerve: Mixed cell infiltrate. Mixed inflammatory cells, with a neutrophilic component, infiltrate the epineurial interstitium.

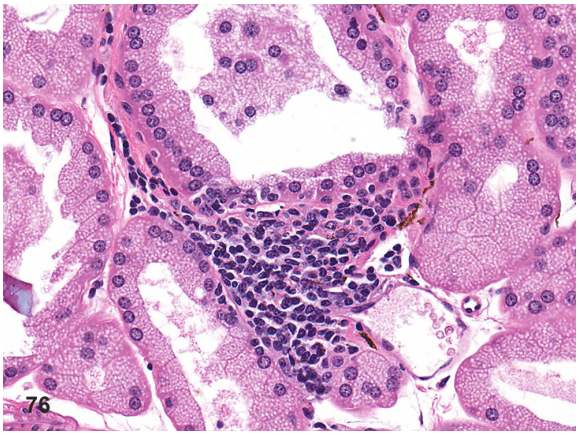


**Fig. 76.** Harderian Gland: Mononuclear cell infiltrate. Mononuclear and mixed inflammatory cell infiltrates are common in the Harderian gland.

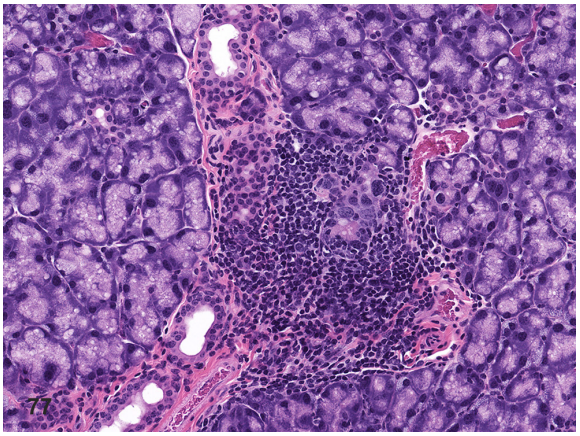


**Fig. 77.** Lacrimal Gland: Mononuclear cell infiltrate. Mononuclear inflammatory cells sometimes infiltrate the connective tissue surrounding glands and/or ducts.

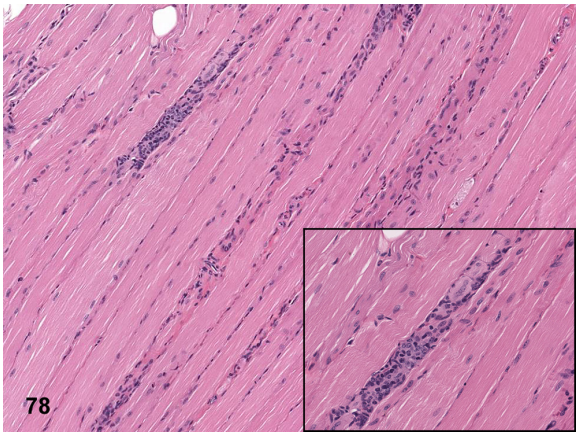


**Fig. 78.** Biceps Femoris Muscle: Myocyte degeneration/regeneration and mixed cell infiltrate. Degenerate myofiber (center of photo) with loss of cross striation and rowing of cells are frequently seen with skeletal muscle myopathy in rasH2-Tg mice. Myopathy occurs in almost every animal in this strain and is occasionally associated with mononuclear or mixed cell infiltrates. Inset: higher magnification.

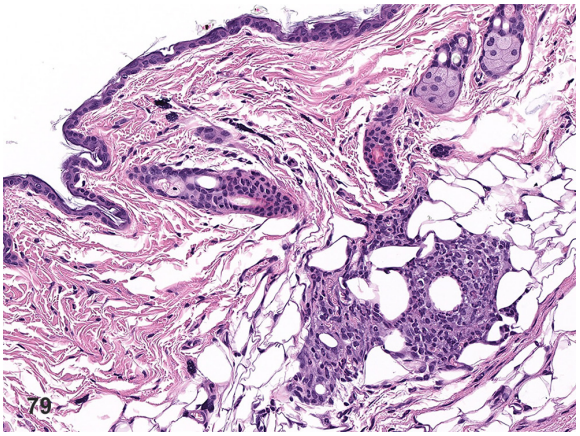


**Fig. 79.** Skin/Subcutis: Mixed cell infiltrate. Mixed inflammatory cell infiltrates are occasionally observed in the skin/subcutis, and in this case are noted focally in the subcutis.

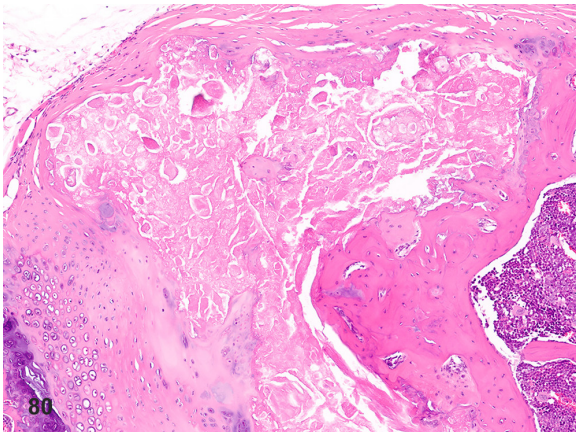


**Fig. 80.** Sternum: Chondromucinous degeneration. Focal pallor and fragmentation of the intersternebral cartilage matrix with loss of chrondrocytes characterizes this occasional finding in the sternum.